Journal of Indian Geomorphology
Volume 11, 2023 ● ISSN 2320-0731
Indian Institute of Geomorphologists (IGI)

# Rapid Climate Change (1981–2021) and Anthropogenic Impact on Landslides in South Sikkim, India

Ria Naskar[1], Arindam Chowdhury[2], Milap Chand Sharma[3] and Sunil Kumar De[1]
[1]*Department of Geography, North-Eastern Hill University, Shillong, Meghalaya 793022*
[2]*Wadia Institute of Himalayan Geology, GMS Road, Dehradun, Uttarakhand 248001*
[3]*Centre for the Study of Regional Development, Jawaharlal Nehru University, New Delhi 110067*
E-mail: desunil@yahoo.com(Corresponding author)

**Abstract:** *This research investigates the complex interplay of the impact of rapid climate change and the frequency of landslides in the highly susceptible terrain of South Sikkim, within a span of forty years from 1981 to 2021. Occurrence of 265 identified and mapped landslides between 1989 and 2022, makes it apparent that the region has become increasingly vulnerable to such events. Geological mapping and GIS analyses underscore the significant impact of various factors such as lithology, tectonics, and river erosion induced slope instability to trigger the landslide events. The climate in Namchi and Ravong areas of Sikkim exhibits considerable dynamism, as evident from the data of the NASA Langley Research Centre (LaRC) POWER Project. Utilising Mann-Kendall analysis, noticeable upward trajectory is identified in temperature and precipitation, indicating climate change over the study period. Correlating landslide occurrences with climatic parameters highlights the predominant role of heavy rainfall, particularly in lower elevations, as a primary triggering factor for landslides. Human interventions, specifically road and other constructions, are identified as exacerbating factors contributing to slope instability. Furthermore, the database is strengthened by Scanning Electron Microscope (SEM) analysis of soil and rock samples, elucidating the material properties influencing landslide susceptibility. Numerical analysis reveals that there is 44% increase in the occurrence of fresh landslides, 2% of landslides were reactivated, 3% experienced expansion, 10% began to shrink, 21% remained dormant and 19% got stabilised between 2019 and 2021-22. This is highlighting the growing concern about the increasing trend of landslides. The numerical and analytical findings offer a valuable insight in developing informed decision-making on the development and formulation of effective risk mitigation strategies in the environmentally dynamic South Sikkim.*

**Keywords:** Rapid Climate Change, Landslides, Mann-Kendall, Scanning Electron Microscope, South Sikkim.

## Introduction

Global warming increases the temperature and frequency of heavy rainfall events, which in turn triggers slope instability and rapid landslides (Gariano and Guzzetti, 2016; Lee *et al*., 2021; Merzdorf, 2020; Tohari, 2018). The frequency of landslide disasters typically increases when different human-induced changes like construction of roads, railway lines, buildings, or increase in agricultural activities, disrupt the mountainous environment, leading to

instability of slopes (Jaboyedoff *et al*., 2016; Jones *et al*., 2021; Sangeeta and Singh, 2023). According to the Climate Change Synthesis Report by IPCC (2023), global surface temperature was 1.09°C higher in 2011-22 than in 1850-1900, which increased the frequency, intensity, and/or volume of intense precipitation and an escalation in heat-related strain (Calvin *et al*., 2023). Heavy rainfall can saturate the soil, reduce its stability and trigger landslides (Martha *et al*., 2015). A rainfall of 50 mm hour$^{-1}$ could trigger landslides due to profound infiltration and percolation of rainwater, facilitated by the geological characteristics of the bedrock leading to the failure of fragile hill slopes in the Himalayan region (Dikshit *et al*., 2020; Kumar *et al*., 2017; Velayudham *et al*., 2021). According to Fischer and Knutti (2015), a global-scale 2°C increase of temperature results in approximately 40% increase in the precipitation extremes exacerbating the risk in areas, prone to landslides. According to the Unified Global Landslide Database, the highest number of landslides occurred in the American and Asian continents, with ~61% of the worldwide landslides occurring after heavy rainfall (Gómez *et al*., 2023).

Deglaciation shortly after the Holocene period made the areas permafrost-free, resulting in significant subsidence (Snook *et al*., 2021). Glacial retreat and permafrost degradation led to the exposure of slopes, which are geologically and morphologically already unstable; inviting rock avalanches and increase in landslide occurrences (Baldis and Liaudat, 2019; Coe *et al*., 2018). Other types of mass movement occur in the lower elevation or fault zones comprising of schist with predominant mineral composition of mica, quartz, feldspar, amphibole and garnet. Landslides in South Sikkim are a common phenomenon owing to the coupled effect of steep slopes, heavy rainfall during Indian summer monsoon, complex geology and tectonic setting (Bhasin *et al*., 2020). Understanding of the mechanisms of rainfall-induced landslides and identifying the influencing factors are essential in prediction and formulation of mitigation strategies in reducing associated risks (Kirschbaum *et al*., 2020). With continuing change in climate impacting the rainfall pattern and temperature rise, there is an urgent need for consistent research, application of advanced technologies and community involvement to strengthen our ability to predict, prevent, and respond to rainfall-induced landslides.

According to the Global Landslide Catalogue, India has recorded the highest fatalities (~27%) from 2007 to 2015 due to landslides. Across various studies (Gaunia, 2022; Kaur *et al*., 2019; Bhasin *et al*., 2023; Bera *et al*., 2019; Sarkar and Mandal, 2021; Sathyanathan *et al*., 2020) on landslide hazard in Sikkim; intensive rainfall, anthropogenic activities (such as road constructions), and seismic activities have been highlighted as primary drivers of landslide occurrences in the region. Increase in extreme rainfall events associated with cloud bursts is one of the primary reasons for landslides. In Sikkim, the risk of landslides along roads is expected to be high during short-duration (24 hrs.) rainfall events with an intensity of 1.82 mm h$^{-1}$ (Koley *et al*., 2019). Rawat *et al*. (2017) investigated the collective impact of geology, intensive rainfall and anthropogenic activities on slope instability. According to Global Seismic Hazard Assessment Program (GSHAP) data, Sikkim falls under a high seismic hazard-prone region and has experienced seismic activities with magnitudes between 5 and 7. These earthquakes induce shallow landslides in the region, causing rock fall, rockslide, soil fall and soil slide (Gupta *et al*., 2015).

Gariano and Guzzetti (2016) reviewed climate change-related literatures since 1990s, and the result clearly showed a research gap linking landslide events with climate

change; compared to the volume of research on climate change itself. The impact of changing climate on geological processes has become increasingly pronounced, potentially leading to alterations in precipitation patterns, temperature regimes and extreme weather events (Buller, 2014). Investigating the influence of climate-related shifts on the susceptibility of regions to landslides is crucial in developing effective strategies on mitigation and adaptation. The primary objective of this research is to assess the correlation between rapid climate fluctuations and anthropogenic impacts, if any, with respect to the occurrence of landslides in the South Sikkim district of the state of Sikkim (India), with an aim to build a comprehensive understanding of the climate drivers and their influence on landslide frequency, magnitude, and distribution within the region.

## Study area

South Sikkim district (88°15'38.74"E to 88°32'4.71"E and 27°4'45.19"N to 27°31'37.39"N) is one of the four districts of the Indian state of Sikkim and is characterised by its hilly terrain, lush valleys, and pristine forests. The state of West Bengal borders the southern part of the study area. The other districts of Sikkim surround the region from three sides. Rangeet river in the west and Teesta river in the east demarcate the boundary of the district. Elevation varies widely, ranging from 400 m in the south to above 5000 m in the north, together with diverse ecological niches varying from subtropical foothills to high-altitude alpine meadows (Government of Sikkim, 2011). It is clear from the DEM image (Fig. 1) that the general slope is from north to south, and the entire district is divided by a mountain ridge

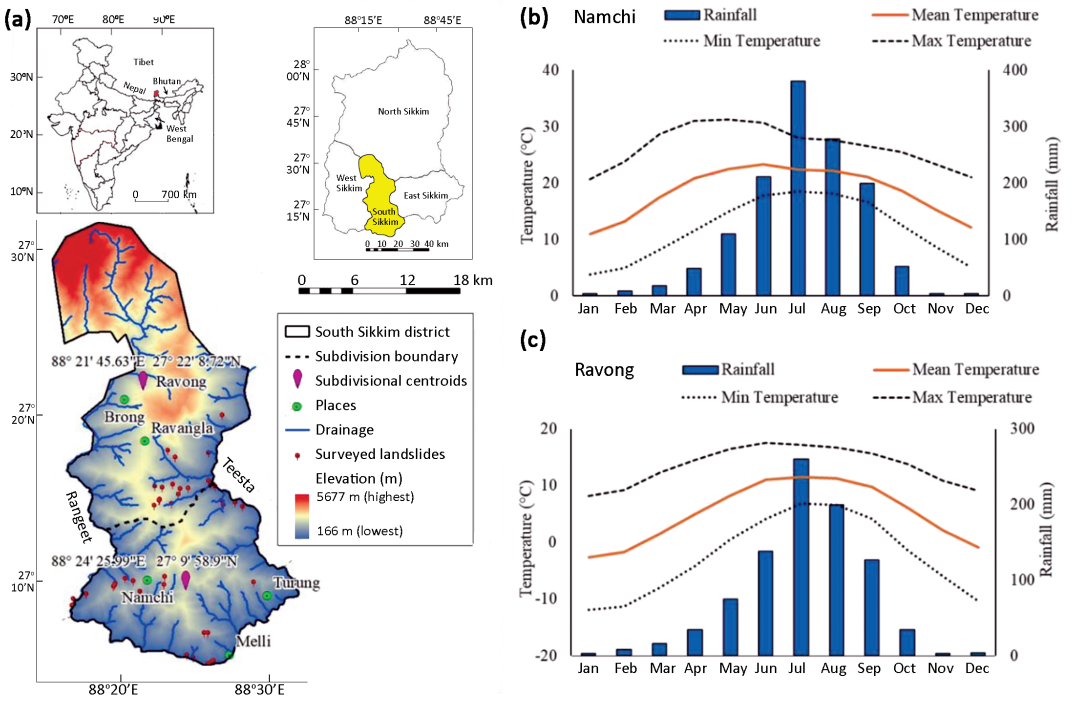


**Figure 1.** (a) Location map of South Sikkim. Climate data has been taken for Namchi and Ravong subdivisions to understand the spatial variation of climatic parameters of the district. Climograph of Namchi (b) and Ravong (c) subdivisions of South Sikkim district showing mean monthly temperature and precipitation data from 1981 to 2021.[Data source: https://power.larc.nasa.gov/data-access-viewer/; accessed on April 4, 2023].

which acts as a water divide for the east and west flowing streams.

The climatic character of the study area is determined by its geographical location on the southern slope of the Himalayas. The low altitude areas experience a subtropical climate with a distinct monsoonal season, while the high-altitude areas have much cooler temperatures. Hence, two different climographs have been shown (Fig. 1b and Fig. 1c) to differentiate the climatic conditions of the two subdivisions — Namchi (located in the south with lower elevation) and Ravong (located in the north with higher elevation). Namchi is the administrative headquarter of the district, ~78 km from Gangtok, capital of Sikkim (Tourism and Civil Aviation Department, 2020) that experiences a warm temperate climate with significantly reduced precipitation in winter and classified as Cwb by Köppen and Geiger (Climate-data.org, 2023). Maximum temperature of the Namchi subdivision (Fig. 1b) ranges from 20–30° C, and minimum from 2–20° C, whereas annual rainfall varies from 1700 mm to 2500 mm. The Ravong region on the other hand receives more than 1200 mm of annual rainfall during the Indian summer monsoon and the temperature ranges from –7° to 15° C (Fig. 1c) and remains snow-covered for a large part of the year.

South Sikkim predominantly comprises of the Eastern Himalayan geological sequence, which consists of sandstone and coal of Damuda formation of the Gondwana Supergroup and the Buxa, Rayong and Gorubathan formations of Daling Group (ENVIS Centre, 2005). These rocks primarily

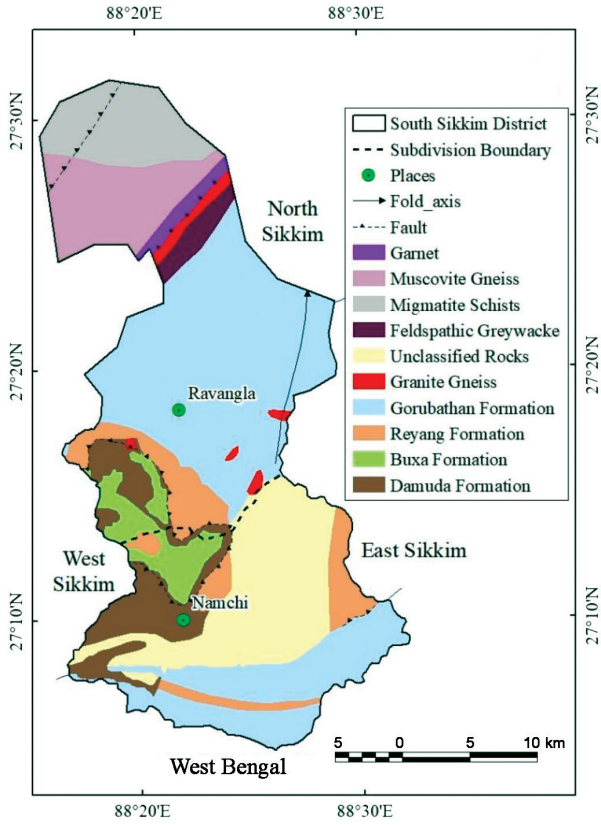


**Figure 2.** Geological map of South Sikkim. (Source: modified after the Geological Survey of India, 2007).

comprise of gneisses, schists, quartzites and phyllites. The Main Central Thrust (MCT) I and II are aligned from west to east in the northern part of the region (Kellett *et al*., 2014; Mottram *et al*., 2014). Damuda formation is separated from the Daling Group of rocks by the Main Boundary Thrust (MBT) in the southwest part. MCT and MBT are active thrusts, and the main Himalayan seismic belt is confined within these thrusts (De and Kayal, 2004). South Sikkim is thus susceptible to earthquakes and lies in Zone IV of Seismic Hazard Zonation of India (Chanda, 2019). Rivers flowing over the low-graded quartzites, phyllites and schists of the Daling Group in the southern section creates wide valleys with gentle slope. The Manpur khola (*khola* depicts a small river) is associated with the phyllites and schists of Daling Group. A major part of the course of the Rangeet river is through the Damuda Group, surrounded by the Buxa formation (Priya *et al*., 2019). Some stromatolite fossils of Carboniferous age are reported from north of Namchi (Sharma *et al*., 2015; Singh and Bajpai, 1990). Buxa formation primarily consists of dolomites, quartzites and shales (semi-anthracite coal), exposed through tectonic windows in the Rangeet valley; overlain by Darjeeling gneisses. River valleys on the northern part of the MCT are characterised by deep, narrow gorges with several knick points. Here, the river courses are mostly structurally controlled.

## Materials and methods

### *Collection of datasets*

#### Landslide events

In absence of any published landslide database from South Sikkim, a comprehensive landslide inventory had to be prepared based on high-resolution images acquired from the Google Earth (GE) platform. Besides the imageries from the European Space Agency's Copernicus program, imageries are provided by Digital Globe, CNES/Airbus, and the Landsat program on the GE platform. The optical and radar imageries captured by the satellites and available on the GE platform offer high-resolution crucial data for detailed analysis of landslide-prone areas. Furthermore, 3D GE features allow comprehensive terrain assessment for landslide studies enabling time-series landslide inventory of the study region between 1989 and 2022. Further, the Landsat series (Landsat TM, ETM+, OLI and Sentinel 2A Multispectral Instrument (MSI) and SRTM DEM were also used to validate the actual location of the landslides.

Using two different approaches landslide activities/events have been recorded. *Firstly*, all visible landslides within the study area were demarcated by polygons on GE for the years 1989 ±2, 1999 ±2, 2009 ±2, and 2019 ±2 (in view of the paucity of images for the exact year, imageries acquired two years prior or after and the target year has been considered) and 2021-22. then Keyhole Markup Language (KML) files of each year were extracted and converted into shape files on ArcMap version 10.1 to delineate the change in the area affected by landslides. The individual shape files were overlain on the satellite image and verified to remove the errors. This process mainly involved visual interpretation of GE images from 1989 onwards and subsequent digitisation of the identified landslide scars. *Secondly*, field visits were conducted in April 2022 and March 2023 to collect data on the geomorphological and geological characteristics of the landslides, including slide location, direction of strike and dip, depth of the regolith and causes of failure. The landslides, identified in the field and through the lens of earth observations, were classified based on their current scenario and character i.e. active (new, shrinking, expanding), dormant or stabilised.

### Climate data

The diverse topography of South Sikkim supports a range of climatic types from subtropical to alpine (Yadava *et al*., 2015). The district has been divided into two subdivisions and point climate data has been collected from the centroids of these subdivisions to cover the spatial extension. The instrumental meteorological record, such as monthly surface air (2 m above the ground), temperature (minimum and maximum) and monthly rainfall for past four decades (1981 to 2021) has been obtained from the NASA Langley Research Centre's (LaRC) POWER Project (https://power.larc.nasa.gov/data-access-viewer/; last access: June 6, 2023).

### *Temporal changes in landslides events*

Temporal landslide changes were studied across four specific years: 1989 ±2, 1999 ±2, 2009 ±2, and 2019 ±2.

### Visual interpretation using Google Earth images

Visual interpretation from Google Earth images includes — a) change in landslide are as within an interval of ten years, b) change in landslide areas at different elevation levels, and c) change in the number of landslides having different slope aspects (direction). While observing these changes in landslides, it is noted that some landslides have stabilised, whereas others have regenerated

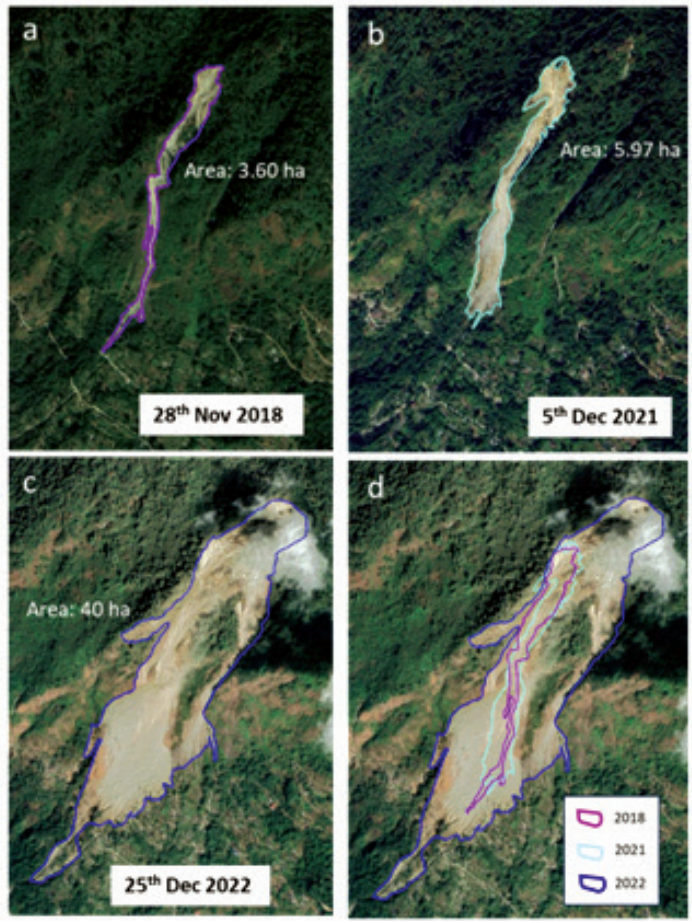


**Figure 3.** (a-c) Landslide change detection identified in Google Earth platform. (d) Polygons are created around the landslide scar and runoff area to track changes in the area of the slide over time.

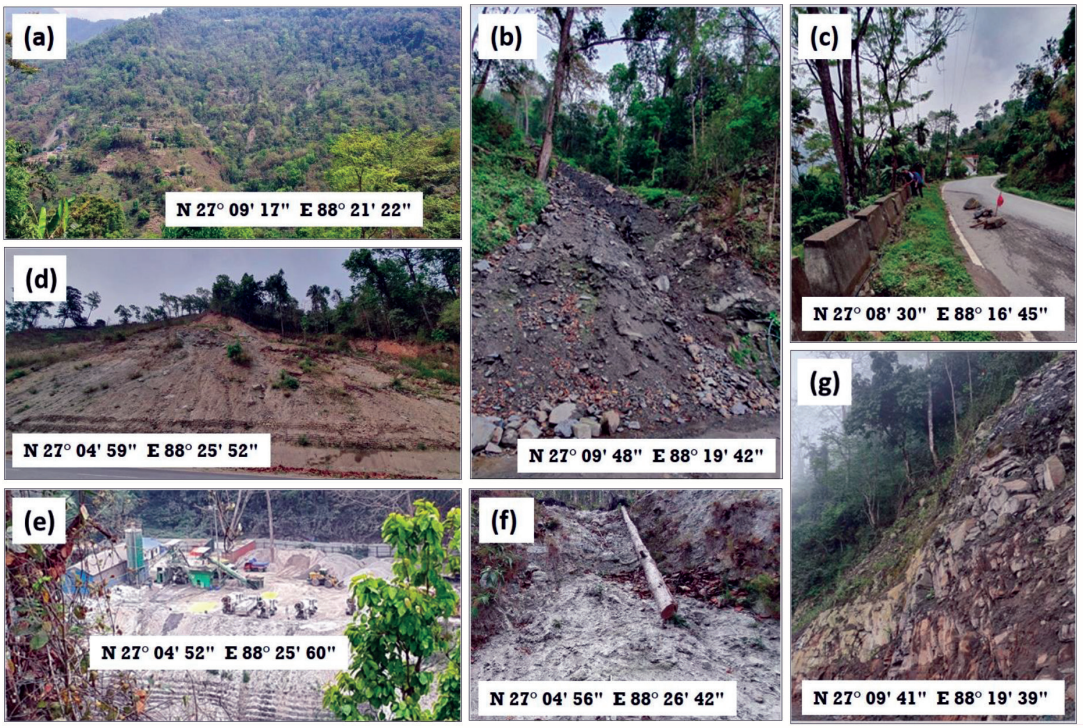


**Figure 4.** (a) Land cover showing moderate to thick vegetation in the area; (b) Dripping and wet conditions observed in the area of debris flow; (c) Subsiding road at risk near Chissopani, Sisney forming transverse cracks; (d) Thick debris material (>3 m) over the rocky exposure near Baiguiney; (e) Sand mining in Rangeet river; (f) Younger loose alluvium near Namchi; (g) Loose debris near Denchong.

after a period of time. An example of areal changes in a landslide is shown in Figure 3.

### Data collection from field and mapping

Figure 4a to 4g highlight the collection of field data through field photographs. This includes the validation of land use/land cover (Fig. 4a), types of slope failure (Fig. 4b), areas near a slope failure (Fig. 4c), thickness of regolith (Fig. 4d), triggering factor(s) for landslides (Fig. 4e), slope angle of the sliding surface, runout distance of slope elevation, rock type, type of denudation, the length-width-depth of landslide scar geometry and type of debris (Fig. 4f-g). Instruments for field surveys included Garmin's hand-held Global Positioning System (GPS), Suunto clinometer, Suunto MC-2 Compass and Carbon Fiber Composites Digital Caliper. The soil samples collected from field were analysed in the laboratory for detailed geotechnical investigation of slope stability. Scanning Electron Microscopy (SEM) images were procured from the JEOL JSM-6360 instrument available as the central laboratory facility with North-Eastern Hill University (NEHU), Shillong.

### *Climate change analysis*

The Mann-Kendall (MK) test along with Sen's slope estimator is applied to analyse the monthly temperature and precipitation variability and determine the trend and magnitude of slope of a regression line on the basis of four decades of monthly climate data from 1981 to 2021.

### Mann-Kendall test

The Mann-Kendall test is a non-parametric statistical test used to assess monotonic trends in time series data (Kendall, 1948; Mann, 1945). The MK test is most appropriately used in exploratory analysis, ideal for identifying stations where significant or large-magnitude changes occur. This test was conducted through the following steps:

In the first stage of the MK test for a time series x1, x2, . . . , xn of length n involves computing the indicator function sgn(xj – xk) where j > k, such that:

$$\begin{aligned} \text{sgn}\,(x_j - x_k) &= 1 \text{ if } x_j - x_k > 0 \\ &= 0 \text{ if } xj - x_k = 0 \\ &= -1 \text{ if } x_j - x_k < 0 \end{aligned}$$

In the second stage, the MK Statistics was computed with the help of the following equation:

$$s = \sum_{k=1}^{n-1} \sum_{j=k+1}^{n} \text{sgn}\,(x_j - x_k)$$

where, is the positive differences minus the negative differences. When is positive, it suggests a tendency for later observations to be larger than the earlier ones. Conversely, when is negative, it indicates a trend where later observations tend to be smaller than the earlier ones.

In the third stage of MK test the variance of was computed by using the following equation:

$$\text{VAR}\,(S) = \frac{1}{18}\left[ n\,(n-1)(2n+5) - \sum_{p=1}^{g} t_p\,(t_p - 1)\,(2t_p+5) \right]$$

where, g = total number of tie groups in the data and $t_p$ = number of data in $p^{th}$ group.

In the final stage, the and VAR (S) were used to compute statistic:

$$Z = \frac{s-1}{[\text{VAR}(s)]^{1/2}} \qquad \text{if } s > 0$$

$$Z = 0 \qquad \text{if } s = 0$$

$$Z = \frac{s+1}{[\text{VAR}(s)]^{1/2}} \qquad \text{if } s < 0$$

A positive ZMK value signifies a tendency for the data to increase over time, while a negative value indicates a tendency to decrease over time. In this study, the MK test was conducted at 99% confidence level. The null hypothesis is rejected if the computed value exceeds 2.58, indicating an increasing or decreasing trend.

### Sen's slope estimation:

Sen (1968) introduced a non-parametric method for estimating the slope of a trend in a dataset that involves computing the pairwise slopes between different data points. The Sen's slope was calculated by using the following formula:

$$Q = \frac{x_j - x_k}{j-k} \text{ for } i = 1, \ldots, N$$

where, $Q_1$ is the estimated slope between data points and for the ith pair; and are the data values at times j and k (where j > k); j and k are indices representing the time or sequence of the data points.

The collected climatic data of four decades was analysed to identify short-term climate patterns and anomalies, including trend identification, and comparison with long-term climate trends. Statistical analysis were used to correlate specific climatic events (e.g., heavy rainfall and temperature fluctuations) with the timing and frequency of landslides.

The seasonal and annual wetness index has also been prepared based on the monthly precipitation data from 1981 to 2021. In this process, the P25 (25th percentile), P50, P75, and P90 have been computed. A year characterised by rainfall falling below the P25 threshold is categorised as an 'extreme dry' year. For years with rainfall within the range of P50 to P25, they are classified as 'dry' years. Similarly, a 'normal' year is defined by rainfall falling between P75 and P50, a 'wet' year between P90 and P75, and any year experiencing rainfall exceeding the

P90 threshold is designated as an 'extreme wet' year.

## Results

*Spatio-temporal distribution of landslides in South Sikkim*

A total of 267 landslides are identified from 1989 to 2022, with the smallest landslide covering an area of 0.006 ha and the largest covering an area of 70.81 ha. Out of the total recorded landslides (majority of the slides originating in 2019), 167 were active during the period 2021-22; 51 achieved complete stabilisation, and 49 landslides were dormant.

In 1989 ± 2, 40 landslides were identified, of which the smallest covered 0.72 ha, whereas the largest covered 39.76 ha. Moreover, 11 new landslides were identified in 1999 ± 2. Among the older landslides, 6 have been found dormant, only 8 slides started shrinking, and others expanded. Since 1989 ± 2, landslide area has increased from 289.26 ha to 371.34 ha in 1999 ± 2. The maximum landslide area recorded in the year 2009 ± 2 was 631.86 ha, comprising of 58 landslides. This peak in landslide activity during 2009 is due to the inclusion of data from 2007 to 2011. The increased landslide affected area observed during this period could be linked to the impact of earthquake of 6.9 Mw magnitude in 2011 (Bhasin et al., 2020). In 2019, approximately 30% of slides stabilised, and 12% began to shrink. However, heavy rainfall during the summer monsoon led to the emergence of 50% fresh slides (Table 1), contributing to an overall increase in the number of slides.

Similarly, during the 2021-22 period, the number of slides rose, with over 44% fresh landslides. The short gap between 2019 and 2021 suggests that a significant portion of the landslides formed in 2021-22 was either freshly formed or reactivated landslides of the previous decade. More than 20% of landslides remained dormant, and 10% started shrinking since 2019.

Utilising SRTM DEM, the entire study area was segmented into altitude zones with 1000 m interval (Fig. 5a). The map illustrates that all landslides occurred below an altitude of 3000 m. Figure 5b and 5c reveal the aspect-wise information of landslides in South Sikkim from 1989 to 2022. The data was organised according to the cardinal directions (N, NE, E, SE, S, SW, W, NW), and the number of landslides in each category was presented for different years. In 1989, landslides occurred predominantly in the SE (47.50%) and S (22.50%) slope aspects. A similar scenario was seen in 1999, when landslides were concentrated in the SE (42.22%) and S (28.89%) directions. Landslides in 2009 were distributed across multiple aspects, with the highest percentage in SE (37.93%) and S (20.69%) aspects. Landslides occurred across various directions in 2019, with a significant percentage in the SE (37.25%), S (31.37%), and E (11.76%). The distribution of landslides in recent years (2021-2022) was predominantly associated with the S (27.54%) and SE (23.35%) slope aspects. Other significant aspects included E (16.77%) and SW (13.17%).

**Table 1.** Percentage variations in the landslide occurrences from 1989 to 2021-2022.

| Period | Stabilised | Reactivated | Dormant | New | Expanding | Shrinking |
|---|---|---|---|---|---|---|
| 1989 to 1999 | 7.84 | 0.00 | 3.92 | 21.57 | 45.10 | 21.57 |
| 1999 to 2009 | 16.22 | 2.70 | 6.76 | 32.43 | 40.54 | 1.35 |
| 2009 to 2019 | 29.33 | 1.33 | 4.00 | 50.00 | 3.33 | 12.00 |
| 2019 to 2021-22 | 19.25 | 2.26 | 21.13 | 44.15 | 3.02 | 10.19 |

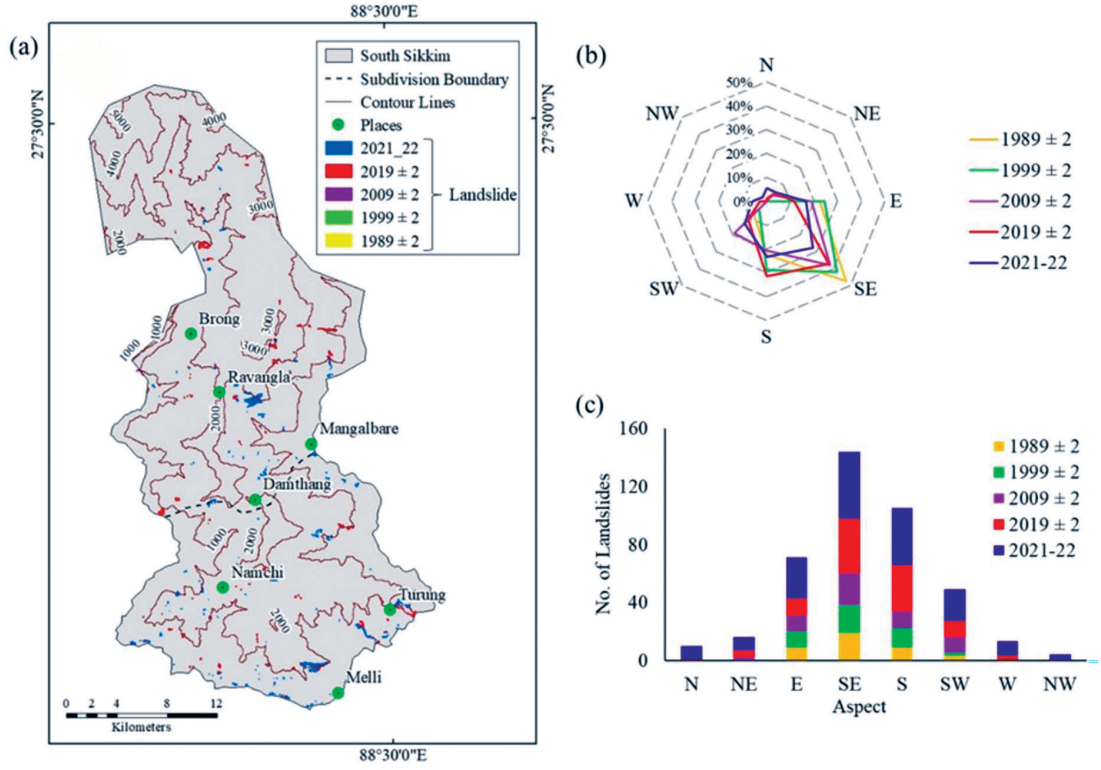


**Figure 5.** (a) Temporal changes in landslide occurrences from 1989 to 2022 in South Sikkim. (b) Percentage distribution of landslides in each aspect category for respective years. The percentages offer a relative measure of the contribution of each aspect to the total landslides in a particular year. (c) Dynamic distribution of landslides across different aspects, with variations in the most affected directions in different years.

Figure 6 represent the number of landslide occurrences (Fig. 6a) and the areal coverage of landslides (Fig. 6b) across different elevation zones from 1989 ± 2 to 2021-22. In 1989, there were 11 landslides covering an area of 73.31 ha within the 1000 m elevation zone, which increased to 94, covering an area of 103.57 ha, by 2021-22 showing a distinct rise in both frequency and area of landslides. In 1989 ± 2, 18 landslides occurred, between 1000 m and 2000 m elevation zone, covering 156.05 ha. The number increased to 67 in 2021-22, affecting an area of 216.88 ha. Over the years there is a notable increase in both landslide frequency and affected area in this elevation band, like the 1000 m elevation zone. There is fluctuation in the number of landslides and significant decrease in the affected area between 2000–3000 m elevation zone during this period. In 1989, there were 11 landslides, covering an area of 59.90 ha which decreased to 6 landslides, covering only 4.75 ha by 2021-22. Maximum landslides in this zone occurred in 2009, covering an area of 90.05 ha. The overall number of active landslides increased from 40 in 1989 to 167 in 2021-22. The total area affected by landslides however, fluctuated, reaching a peak of 631.86 ha in 2009 and then decreasing to 325.20 ha in 2021-22.

The data collected from GE illustrated a general trend of increase in landslide occurrences from 1989 to 2022 (Fig. 6a), especially in lower elevation zones (Fig. 6b). The elevation of South Sikkim ranges from 200 m to 5000 m, but the concentration

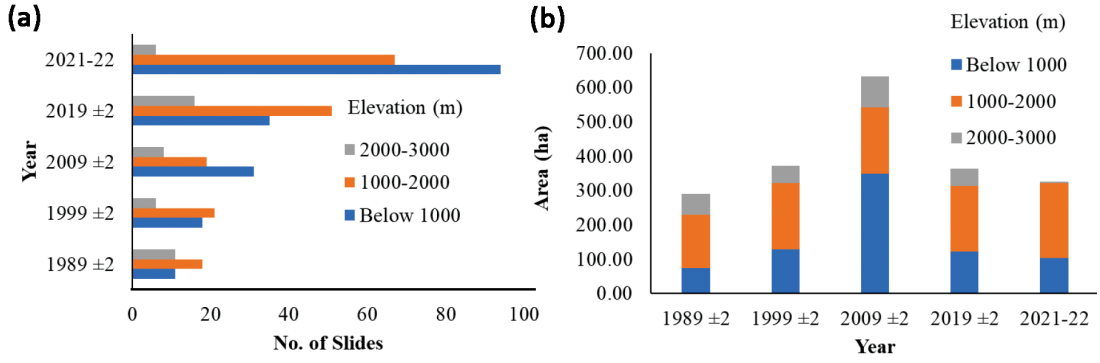


**Figure 6.** (a) Change in landslide occurrences across different elevation zones from 1989 to 2022 (b) Alteration in landslide area (in ha) across different elevation zones from 1989 to 2022.

of landslides is primarily within 3000 m. Majority of the landslides occurred below 1000 m and between 1000 m to 2000 m altitude, indicating a higher susceptibility to landslides in zones with increased human interference. In South Sikkim, regions such as Namchi, Ravangla, Damthang, Turung, Mamring, Melli, and Mangalbare, among others, are particularly impacted by landslide activity, attributed to a combination of anthropogenic and natural factors.

*Climate change scenario in South Sikkim*

Precipitation and temperature records of Namchi and Ravong stations from 1981 to 2021 are taken into consideration to assess the trends within South Sikkim (Fig. 7). A positive and negative Rainfall Anomaly Index indicates higher-than and lower-than-average rainfall respectively.

At Namchi (Fig. 7a), there seems to be a trend of negative anomaly from 1983 to around 2009, except in the year 2007. However, from 2010 onwards, there was a shift to predominantly positive anomalies, indicating higher rainfall than the average, with a significant increase, particularly in 2020 and 2021. It suggests an overall change in rainfall pattern in the region over the observed years.

Ravong rainfall data (Fig. 7b) shows a negative Rainfall Anomaly Index from 1982 to 2009, but since 2010 the region has experienced above-average rainfall. Like Namchi, Ravong also witnessed its highest recorded rainfall in 2020 (2056.64 mm) and the lowest in 1993 and 1994 (448.24 mm). During spring, the minimum rainfall occurred in 1991 (5.27 mm), while the maximum was observed in 2020 (105.47 mm). Similarly, summer rainfall peaked in 2020 (428.91 mm), contrasting with its lowest value in 1993 (105.47 mm). The autumn season also reflected a similar pattern, registering the highest rainfall in 2020 (133.59 mm) and the lowest in 1994 (15.82 mm). The region experienced completely dry winters with no rainfall for 21 years, except for the year 2019 which received the maximum winter rainfall of 21.09 mm. After 1990, nearly every season consistently experienced low levels of rainfall, indicating a prolonged dry spell in Ravong. The same is illustrated in Figure 8, displaying Ravong's wetness index spanning from 1981 to 2021.

By employing percentile calculations on precipitation data, distinct thresholds can be established to categorise specific years as either dry or wet. Using the annual rainfall data for Namchi, five distinct categories of

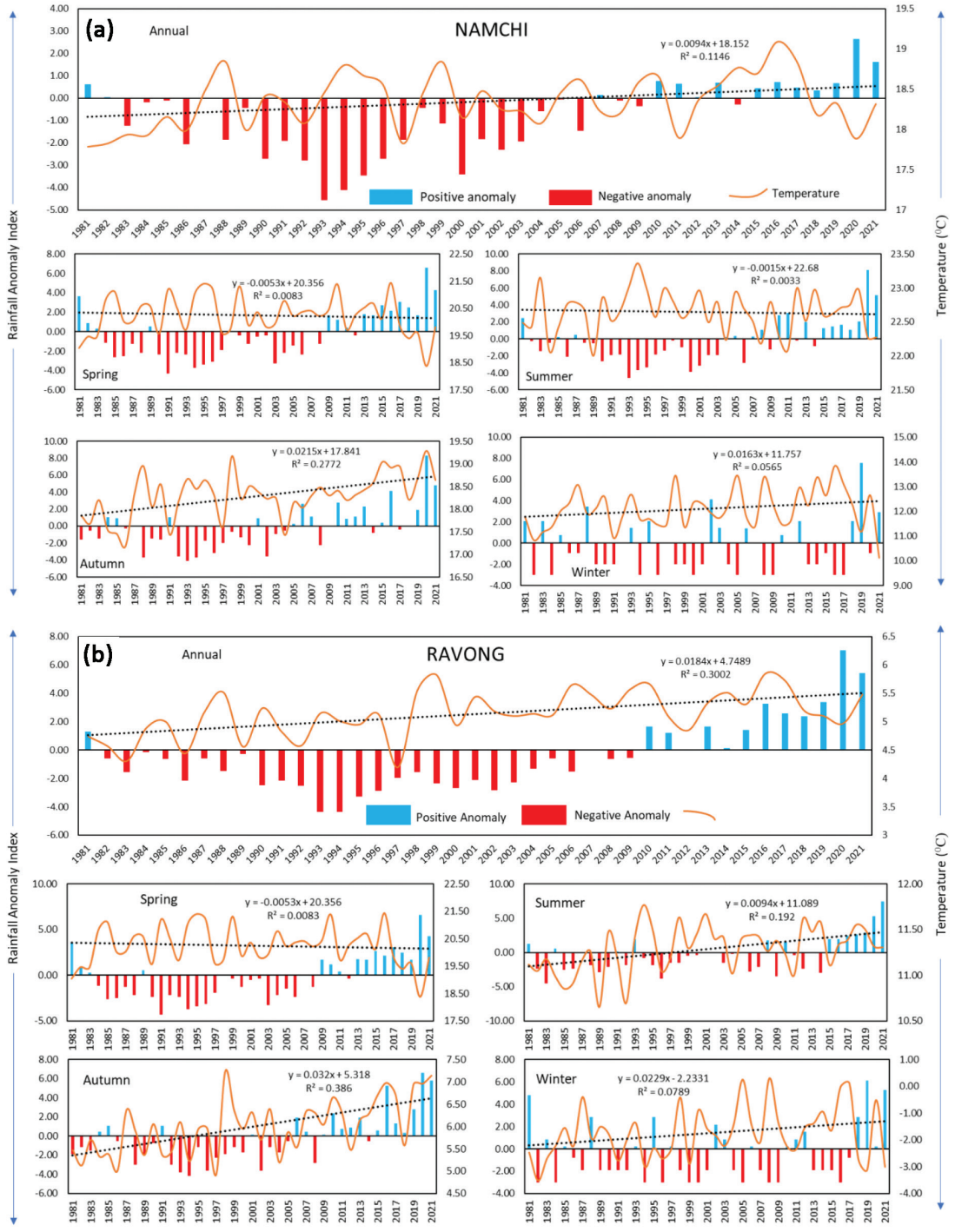


**Figure 7.** Annual and seasonal Rainfall Anomaly Index and Temperature trend of (a) Namchi and (b) Ravong from 1981 to 2021.

wetness (Fig. 8a) have been established — extreme dry (rainfall below 1041.51 mm), dry (rainfall ranging from 1041.51 to 1316.42 mm), normal (rainfall between 1316.42 and 1566.21 mm), wet (rainfall between 1566.21 and 1772.93 mm), and extreme wet (rainfall exceeding 1772.93 mm). Maximum fluctuation in seasonal rainfall was seen from 2000 to 2009. Throughout this period, there was a consistent occurrence of extremely dry conditions, with the exception of above-average rainfall during the autumn and winter seasons. In 2020, Namchi experienced an exceptionally high rainfall, reaching nearly 3000 mm, a phenomenon rarely observed in this region. On the contrary, 1993 marked the driest year with a meagre 664 mm of precipitation. The years 1986,

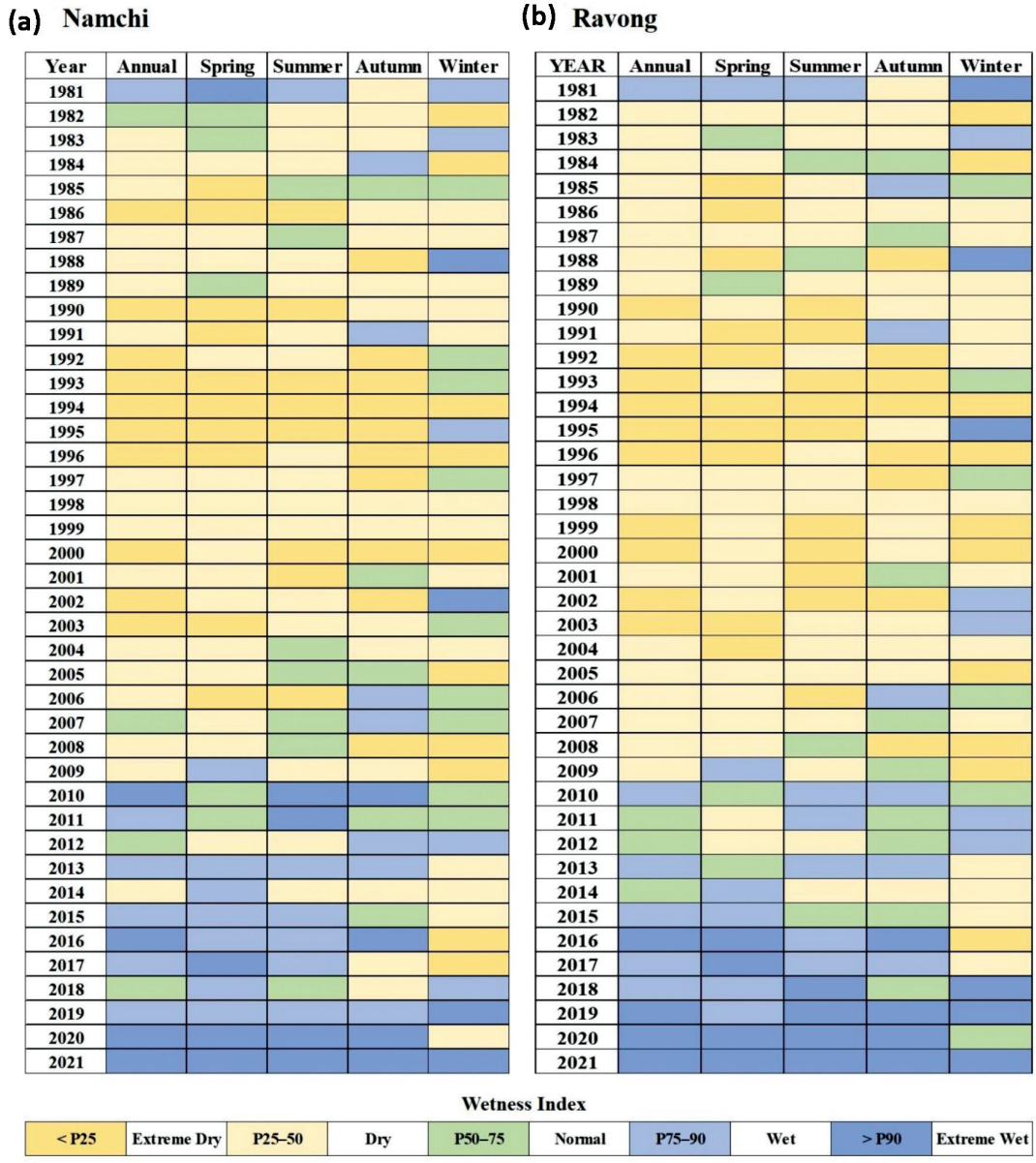


**Figure 8.** Annual and seasonal wetness of (a) Namchi and (b) Ravong, based on the monthly rainfall from 1981 to 2021.

1990, 1992 to 1996, 2000, and 2002 to 2003 were characterised by extreme dryness. Interestingly, many of these years received winter rainfall, possibly an indication of climate change.

The annual precipitation data of Ravong has been similarly categorised into five different classes (Fig. 8b) — extreme dry (below 669.73 mm), dry (669.73 to 889.88 mm), normal (889.88 to 1104.79 mm), wet (1104.79 to 1412.23 mm) and extreme wet (above 1412.23 mm). It is observed that, the years 2016 and 2019 to 2021 were particularly notable for being extremely wet, receiving over 1400 mm of rainfall. Conversely, 1990, 1992 to 1996, 1999 to 2000, and 2002 to 2003 were extremely dry, receiving less than 670 mm of rainfall. Prior to 2006, majority of the autumn seasons remained dry, with less than 50 mm of rainfall. But since 2006, autumnal rainfall has been on the rise. Furthermore, in the last decade, from 2010 to 2013 and from 2018 to 2021, there has been notable increase in winter rainfall.

Out of the 41 years data analysed, 27 years (65%) have been recognised as having extreme dry to dry condition based on the wetness index of Namchi and Ravong (Fig. 8a and 8b). Approximately 60% of the 41-year timeframe experienced less than 50% of the average rainfall during the spring, summer, and autumn seasons. It is observed that, 55% of the winter seasons within this period exhibited very dry conditions. Only 20% to 25% of the time span experienced wet conditions. South Sikkim has exhibited a rising trend in rainfall since 2010, marking a shift from the preceding three decades characterised by dry spells.

The southern part of South Sikkim (Namchi subdivision) experiences a tropical monsoonal climate, whereas the northern part (Ravong subdivision) has a temperate climate. Consequently, there is a decline in rainfall from the south to the north. Table 2 and Table 3 show the results of the Mann-Kendall (MK) test and Sen's Slope for different seasons, representing the trend analysis for the specified parameters (rainfall and temperature) during these seasons for Namchi and Ravong respectively.

Where, spring (Mar-May), summer (Jun-Aug), autumn (Sep-Nov) and winter (Dec-Feb), '↑' increasing trend, '–' no trend, * significance level ($\alpha$) = 0.01

Spring, summer, and autumn seasons show an increasing trend in rainfall, while winter shows no such trend for both the regions. Overall, there was an increasing trend in the annual rainfall of South Sikkim during this period. Sen's slope shows this rising rate is the maximum for annual rainfall and the second highest for the summer season. However, the temperature analysis using the Mann-

**Table 2.** Mann-Kendall ($Z_{MK}$) test for statistical trend analysis of long-term temperature and precipitation and Sen's Slope analysis shows the rate of change in precipitation (mm) and temperature (°C) for the period 1981-2021 in Namchi, South Sikkim

| NAMCHI | | | | | | | | | | |
|---|---|---|---|---|---|---|---|---|---|---|
| Season | Rainfall (mm) | | | | | Temperature (°C) | | | | |
| | $Z_{MK}$ | Y | $R^2$ | Sen's Slope | Trend | $Z_{MK}$ | Y | $R^2$ | Sen's Slope | Trend |
| Spring | 3.83 | 1.5615x – 3065.8 | 0.32 | 1.76 | ↑ | –0.19 | –0.0053x + 30.91 | 0.01 | 0 | – |
| Summer | 3.28 | 3.7507x – 7215.5 | 0.28 | 3.48 | ↑ | –0.29 | –0.0015x + 25.65 | 0.00 | 0 | – |
| Autumn | 3.29 | 1.7486x – 3413.9 | 0.30 | 1.55 | ↑ | 3.17 | 0.0215x – 24.78 | 0.28 | 0.02 | ↑ |
| Winter | 0.10 | 0.055x – 104.92 | 0.01 | 0.00 | – | 1.60 | 0.0163x – 20.50 | 0.06 | 0.02 | ↑ |
| Annual | 3.65 | 21.177x + 871.69 | 0.34 | 19.08 | ↑ | 2.19 | 0.0094x – 0.48 | 0.11 | 0.01 | ↑ |

Kendall test presents a different picture. No discernible trend is observed in temperature of Namchi for the spring and summer seasons, whereas there is an increasing trend in autumn and winter temperatures, although at a relatively moderate rate. Despite Ravong having lower temperatures than Namchi, there is an observed upward trend in temperature from 1981 to 2021. The autumn season has displayed the most significant upward trend in temperature. Moreover, the rate of precipitation increase is notably higher than the rate of temperature change in the district. Although the rate of temperature increase is minimal, it does reflect the current trend of global warming.

The climate change pattern in South Sikkim is evident through the discernible increasing trends in rainfall and temperature. Over the specified period of 1981–2021, there is a noteworthy rise in precipitation, reflecting changes in the region's precipitation pattern. Concurrently, temperatures have shown an upward trajectory, indicating a warming trend. Intense and often unpredictable downpours have become more frequent in the last few years in the study area. In 2020 and 2021, the maximum extreme rainfall events occurred in May and June, while in 2022, such events took place in September and October. These extreme rainfall events contribute to severe landslides and flooding. Heavy rainfall in June 2022 caused a huge landslide that blocked the road to Jorethang. On September 1, 2022, heavy downpours resulted in landslides that impacted more than 40 villages. Since 2020, the road near Melli Bazar washes out during the monsoon season every year due to landslides.

Where, spring (Mar-May), summer (Jun-Aug), autumn (Sep-Nov) and winter (Dec-Feb), '↑' increasing trend, '–' no trend, * significance level (α) = 0.01

*Correlation between climatic and anthropogenic factors of landslide*

Majority of landslides within the Himalayan belt are triggered by rainfall, contributing to approximately 15% of the world's rainfall-induced landslides (Dikshit *et al*., 2020). If climate change predictions manifest as anticipated, then there is a foreseeable intensification of landslide occurrences in conjunction with population growth in the Himalayan region. The risk of slope instability amplifies significantly in areas which are developing fast like South Sikkim, characterised by extensive agricultural activities, population surges, and heightened scale of land exploitation. Field observations during 2022 and 2023 also show that a significant concentration

**Table 3.** Mann-Kendall ($Z_{MK}$) test for statistical trend analysis of long-term temperature and precipitation and Sen's Slope analysis shows the rate of change in precipitation (mm) and temperature (°C) for the period 1981-2021 in Ravong, South Sikkim.

| RAVONG | | | | | | | | | | |
|---|---|---|---|---|---|---|---|---|---|---|
| Season | Rainfall (mm) | | | | | Temperature (°C) | | | | |
| | $Z_{MK}$ | Y | $R^2$ | Sen's Slope | Trend | $Z_{MK}$ | Y | $R^2$ | Sen's Slope | Trend |
| Spring | 4.16 | 1.5932x – 3146 | 0.42 | 1.56 | ↑ | 0.40 | 0.0055x – 6.23 | 0.013 | 0 | – |
| Summer | 3.50 | 3.2325x – 6269.2 | 0.35 | 2.97 | ↑ | 2.44 | 0.0094x – 7.45 | 0.19 | 0.01 | ↑ |
| Autumn | 3.74 | 1.3438x – 2634.5 | 0.36 | 1.20 | ↑ | 4.07 | 0.032x – 58.13 | 0.39 | 0.03 | ↑ |
| Winter | 0.81 | 0.0795x – 154.41 | 0.03 | 0 | – | 1.61 | 0.0229x – 47.58 | 0.08 | 0.02 | ↑ |
| Annual | 4.08 | 18.649x – 36417 | 0.42 | 17.14 | ↑ | 3.40 | 0.0184x – 31.64 | 0.30 | 0.02 | ↑ |

of landslides occurs more frequently and with greater magnitude in close proximity to the road network (both highways and rural roads), signifying increased slope instability primarily attributable to human interventions.

There is a considerable change in landslide area within 1000 m to 2000 m elevation zones (Fig. 6). It is mainly because this elevation zone faces the most transition due to climate change. The number of landslides increased within 1000 m elevation, though the area of landsides has not increased much because these slides are shallow in nature and have limited regolith cover. The occurrence of shallow landslides, which typically happen annually or biennially, have significantly increased in recent years (2021–22) due to frequent extreme rainfall events. The landslide area underwent a significant shift (increasing order), from 371.34 ha in 1999 ± 2 to 631.86 ha in 2009 ± 2, primarily attributed to dry spell followed by intense rainfall in 2010. This decade was marked by reduced monsoon rainfall and more than average precipitation during the autumn and winter seasons. Alternating wet and dry conditions cause soil to expand and contract respectively. This cycle of expansion and contraction weakens the soil structure over time, making it more susceptible to sliding. Fluctuating rainfall pattern alongside increasing temperatures (from 2001 to 2009) create zones of weakened stability, fostering gradual failure that eventually culminates in significant landslides.

During wet periods, the soil absorbs water and becomes saturated. In the following dry periods, the excess water may not evaporate or drain quickly, leading to prolonged saturation. Saturated soil is more prone to landslides as it becomes heavier and undergoes liquefaction. In 2021–22, there was a notable surge in the number of landslides, with a total of 167 active slides, among which 116 were freshly formed after 2019. This increase is attributed to the heavy rainfall experienced in 2020. Autumn and winter temperatures showed an increasing trend, especially after 2005. Warmer and drier weather creates ideal conditions for more desiccation, potentially leading to the formation of ground surface cracks at points where failure begins (Ganepola and Jayawardena, 2021). These cracks become the pathways for water to seep-in during wet periods, enhancing pressure build-up and weakening the stability of soil in the process. As these cracks repeatedly open and close with changing seasons and increased rainfall, the permeability of soil rises, creating zones of reduced strength. This gradual weakening can trigger progressive failure, ultimately culminating in significant landslides.

Human activities such as construction, mining, or deforestation can alter the natural stability of slopes. The risk of landslides significantly increases due to the combined impact of rainfall and road cuts (Ansari *et al*., 2020; Pradhan *et al*., 2022). In 2009 and 2021–22, there was a shift in landslide concentration from the S and SE directions to multiple directions, indicating human interference in addition to rapid climate change. Currently, a significant number of landslides are concentrated along roads due to fresh road cutting, road widening, settlement growth etc. within the study area. An instance of such landslides has been observed in Denchong near Namchi on the northeastern slope, lying opposite to the direction of monsoonal wind (Fig. 9). This particular landslide experienced significant reactivation in October 2021, following its initial occurrence in 1987. The reactivation was primarily attributed to cut-and-fill construction for roads and its widening activities. Consequently, the landslide intercepted the Namchi-Wak-Sikkim Road at three distinct elevations (1225 m, 1092 m, and 948 m), leading to the disruption of

communication. Additionally, within the landslide boundary (Left Panel, Fig. 9), the process of hillslope-channel coupling is manifested as a rill enlarges and transforms into gully (Fort *et al*., 2010). Signatures of soil creep were also seen during field investigations, manifested through bending of trees (Middle Panel, Fig. 9). Further, the annual occurrence of this major landslide within the study area can be described through soil micromorphology studies (Right Panel, Fig. 9) carried out on Scanning Electron Microscope (SEM).

The SEM images (right panel, Fig. 9) provide detailed information about the surface topography of samples collected from the Denchong slide from points A, B and C (left panel, Fig. 9). The mean particle diameter

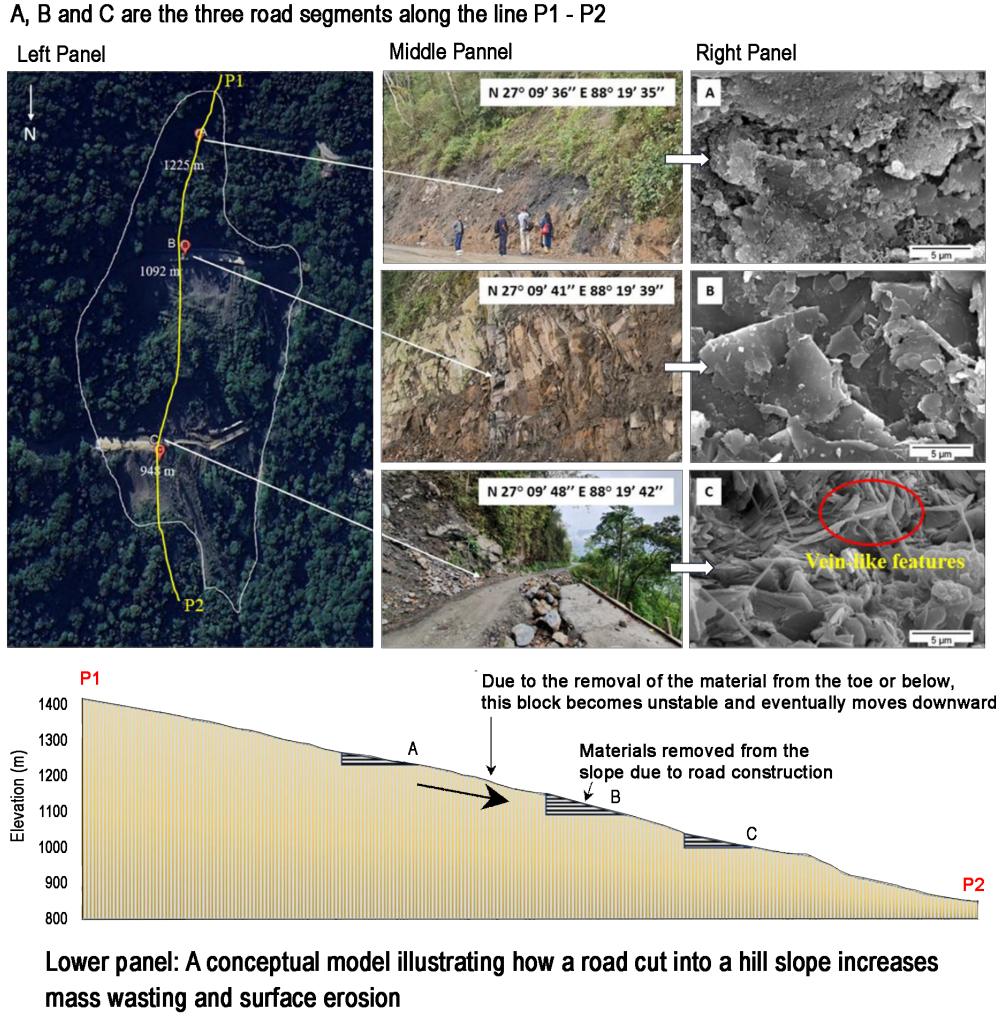


**Figure 9.** Left Panel showing the Google Earth Imagery of Denchong Landslide near Namchi. The topmost section is identified as the crown or prominent scarp, labelled 'A'. The middle part is denoted as 'B', and the lower part, constituting the tail beneath which the toe of the slide is situated, is marked as 'C'. The Middle Panel displays field images (captured on April 10, 2022) of the same slide from three distinct elevation points, where it cuts the 'Namchi-Wak-Sikkim' road three times. The Right Panel exhibits SEM images of samples collected from points A to C, from the top to the bottom of the landslide. In the Lower Panel, a long profile is drawn along the line P1-P2, with a schematic presentation showing how road cutting makes the slope unstable.

extracted from SEM image A (top) measures 0.14 μm, while for image B (middle), it is 0.22 μm, and for image C (bottom), it is 0.81 μm. A transverse crack is visible in the lower part of the slide, serving as an indicator of extensive weathering. Biological weathering is pronounced in this area due to the presence of water, supported by the observation of vein-like features in SEM Image C. Cutting into a hillslope for road construction removes support from the slope's base, increasing landslide risk. The exposed soil and rock become more susceptible to erosion from rainfall and surface runoff, which can be exacerbated by the road channelling water flow. This dual impact destabilises the slope, leading to increased mass wasting and surface erosion (lower panel, Fig. 9).

Water interacts uniquely with coal as compared to other rocks, impacting pore pressure and groundwater flow. These dynamics affect coal seam stability, crucial for slope integrity and landslide risk. This is seen in the Denchong landslide involving phyllite, gneiss, and coal. Coal is more prone to weathering than the harder rocks, which over time had a negative impact on the stability of coal, leading to subsequent slides post-1987. During road widening, rainwater infiltration exacerbates soil cracking due to insufficient drainage through dissected hard rock layers. In 2021 prolonged heavy rainfall from May to October intensified water infiltration, triggering debris flows and rockfalls within the coal zone. Seepage further compromised block integrity, exacerbating slope instability.

## Discussion

### *Comparison of landslide distribution and dynamics*

A landslide database on a national and regional scale can be a useful tool for landslide management and the early warning system (Devoli *et al*., 2007). Detection and monitoring of pre-existing landslides are important in hilly areas for disaster avoidance, preparedness, and mitigation (Mondal and Mandal, 2019; Rosin and Hervás, 2005). Table 4 shows the temporal and spatial distribution of landslides, presenting significant information extracted from GE imagery, documenting landslides from 1989 ± 2 to 2022 ± 2. Temporal changes in landslide area exhibit a gradual increase from 1989 ± 2 to 1999 ± 2, followed by a sudden doubling of the landslide area from 1999 ±2 to 2009 ± 2. This notable increase may be attributed to changes in climate and tectonic activities. Although the landslide area decreased in 2019, the number of slides doubled compared to the previous decade. In the recent period of 2021–22, the number of landslides significantly rose, probably due to the high precipitation rates across the entire region.

Analysing the data from Table 4 indicates that majority of the slides occurred on the windward side, particularly in the SE, S, E, and SW directions. Conversely, the leeward side (N, NW, W, NE) experienced fewer landslide activities due to less rainfall. S and SE-facing slopes are more exposed to prevailing monsoon winds (Dhar *et al*., 1984), and receive direct sunlight (Hamal *et al*., 2021) resulting in increased weathering and weakening of rock and soil, facilitating the landslides. Moreover, changes in climate pattern in recent years, such as increase in the rainfall intensity or temperature, influence landslide occurrences in this region. Landslides can alter the landscape and create conditions that make the area more susceptible to landslides. Historical records indicate a propensity for landslides on S and SE-facing slopes, making the slope more prone to landslide recurrence (Zhang *et al*., 2016). Consequently, from 1989 to 2022, over 50% of the total landslide occurrences have been concentrated within this specific zone.

**Table 4.** Landslide Distribution and Temporal variation of landslides in South Sikkim (1989 to 2021–22).

| 1989 ± 2 | | Years | | | | |
|---|---|---|---|---|---|---|
| | | 1999 ± 2 | 2009 ± 2 | 2019 ± 2 | 2021-22 | |
| No. of Landslides | | 40 | 51 | 74 | 150 | 265 |
| Area (ha) | | 289.26 | 371.34 | 631.86 | 363.90 | 325.20 |
| No. of Active Landslides | Newly formed | 40 | 11 | 24 | 75 | 117 |
| | Expanding | 0 | 23 | 30 | 5 | 8 |
| | Shrinking | 0 | 11 | 1 | 18 | 27 |
| | Reactive | 0 | 0 | 2 | 2 | 6 |
| No. of Dormant slides | | 0 | 2 | 5 | 6 | 56 |
| No. of Stabilised slides | | 0 | 4 | 12 | 44 | 51 |
| Aspect-wise No. of Landslides | | SE (19), S (9), E (9), SW (3) | SE (19), E (13), S (11), SW (2) | SE (22), S (12), E (11), SW (11), NE (2) | SE (38), S (32), E (12), SW (11), NE (5), W (3), N (1) | SE (46), S (39), E (28), SW (22), NE (9), W (10), N (9), NW (4) |
| Elevation Zone-wise No. of Landslides | < 1000 m | 11 | 18 | 31 | 35 | 94 |
| | 1000-2000 m | 18 | 21 | 19 | 51 | 67 |
| | 2000-3000 m | 11 | 6 | 8 | 16 | 6 |
| Elevation Zone-wise Landslide area (ha) | < 1000 m | 73.31 | 128.97 | 348.15 | 121.72 | 103.57 |
| | 1000-2000 m | 156.05 | 191.64 | 193.66 | 192.18 | 216.88 |
| | 2000-3000 m | 59.90 | 50.73 | 90.05 | 50.00 | 4.75 |
| Type of Landslides | | Debris flow (maximum), Rockfall, and Creep | | | | |

Source: All data have been extracted through Google Earth (GE) imagery, SRTM DEM and by using ArcMap 10.1.

Landslides (particularly debris flow) extending to the toe part near a river or stream exhibit persistent instability (Jana, 2002). Such slides occur almost every year, especially during monsoons, if there is a substantial thickness of regolith. One of the giant landslides in South Sikkim near Pathing, is the Ravangla slide (Fig. 3), extending downhill into the Rangpo Khola, eventually joining the Tista river near Sinchuthang. Figure 10a reveals substantial amount of regolith in the slide, and the stream at the base carrying away the debris, contributing to the instability of this landslide. Before 2021, the mass wasting activity in the area was relatively subdued, but in the following monsoon season the 2022, it became more dynamic. The toe of the landslide extended to the Rangpo Khola (Fig. 10b), resulting in erosion along two roads connecting Ravangla and Pathing. Additionally, 76 households (Fig. 10c) were relocated from this location as the area became unsuitable for habitation. Photograph of the entire landslide is shown in Figure 10d. The landslides near Ben Khola (Fig. 11a) serve as additional examples of how these events impact daily life and disrupt road communication. These slides occur at a relatively high frequency, with 2 or 3-year recurrence interval, causing damage to NH 510 (Fig. 11b), which connects Namchi to Ravangla.

In most surveyed landslides, initiation or reactivation of slides occurred primarily after heavy rainfall (Table 5). Unsuitable geological and geomorphic conditions, along with the absence of a proper drainage system contributed to the reactivation of landslides

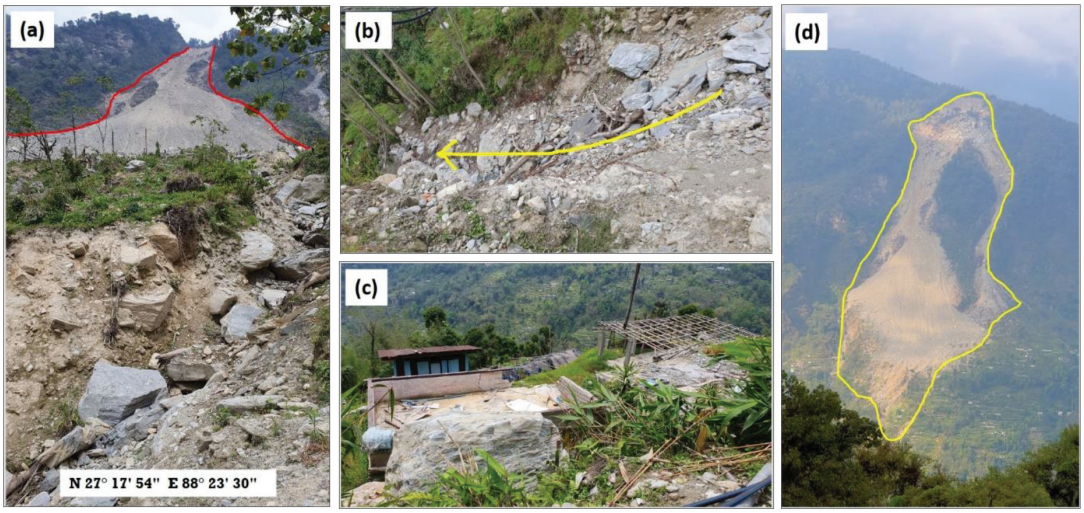


**Figure 10.** Field photograph of Ravangla landslide (near Pathing). There is a significant accumulation of debris with a regolith thickness >6 m, and the length of the slide extends beyond 1550 m (b) The toe of the landslide extends downward, reaching the Rangpo Khola (c) Houses have been affected, and residents were relocated from this area (d) Photograph showing the entire landslide of Ravangla (April 25, 2023).

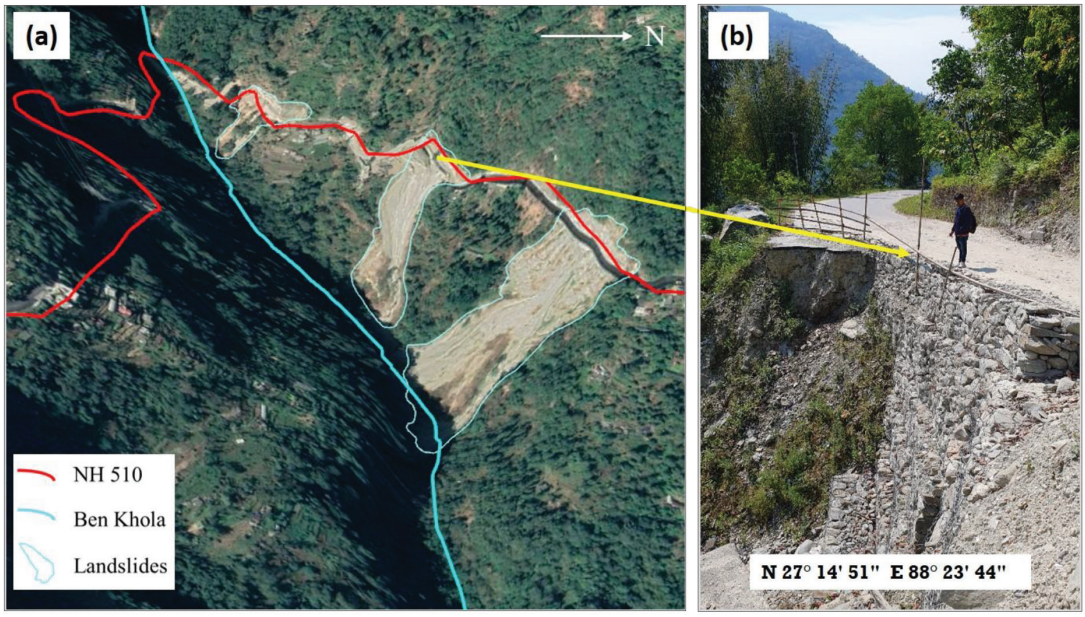


**Figure 11.** (a) Landslides near Ben khola, as observed in GE imagery (December 25, 2022), have caused damage to NH 510 (a spur road of NH 10). Note: The entire NH 510 was marked thoroughly using the tracking mode of the GPS Essential and SW Maps application. (b) Photograph captured in the field depicting the same landslide near Ben khola, showing an impact on the guard wall.

during a period of heavy rainfall (Dobrescu *et al*., 2011). Occasionally, the slides are triggered after road cutting along the toe of landslide. In some cases, the combination of rainfall and road cutting contribute to landslides. The initiation of slides during

the monsoon season, especially following episodes of intense rainfall, indicates the significant role of water as a trigger to debris slides (Sharma *et al*., 2010). Debris flow and debris slides constitute the primary and most prevalent modes of slope failure in the study area, collectively accounting for over 65% of occurrences (Fig. 12a). Another significant type of slope failure in the region is rockfall.

Sikkim has the steepest mountain slope in India, as the width of the Himalayas is narrowest here (Schaller, 1977). Steep slopes are more susceptible to erosion as well as landslides. In this study, we have surveyed 35 active landslides in South Sikkim between 2022 and 2023. Among these, majority of the landslides occurred on slopes greater than 45º. Another study in the Sikkim Himalayas (Rawat *et al*., 2017) also determined that the slopes ranging from 46° to 75° are identified as most susceptible to landslides. Figure 12b clearly illustrates that over 75% of the surveyed landslides occurred on slopes with angles exceeding 40°. Sarkar and Mandal, 2021 stated that almost 40% of the landslides of South Sikkim are found within the 'high landslide risk zone'. The findings of this study indicates that landslides are concentrated in

**Table 5.** Field-investigated parameters of surveyed landslides between 2022 and 2023..

| | |
|---|---|
| No. of surveyed landslides | 35 |
| Slope (°) | 29–80 (average slope: 50) |
| Rock types | Gneiss, schist, phyllite, sandstone, coal |
| Triggering factors | Rainfall, cut-and-fill processes for the construction of roads, bridge construction, mining activities (coal), poor drainage system |
| Failure types | Debris-slide (rotational slide and translational slide), debris flow, slip, creep, rockfall (wedge failure) |
| Regolith thickness (m) | 2–5, (>5 m) |
| Land use/ land cover | Roads (highways and rural), forests, settlements, plantation or agricultural lands, etc. |
| Length (m) | 10–1500 |
| Width (m) | 4–500 |

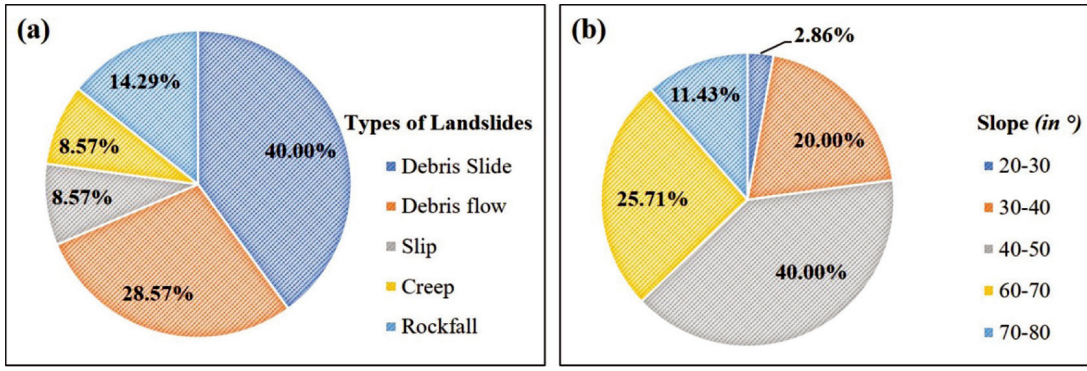


**Figure 12.** (a) Types of surveyed landslides. Note: debris slides are mainly rotational and translational slides; debris flows are primarily found near the spring flow or slopes with poor drainage system; slips are generally complex slides, fast movement of soil mass or rock along steep slope; creep manifests as a gradual downward movement of earth mass along slopes; and rockfall incidents are commonly identified in areas where bedrock has been exposed, with a majority of falls attributed to wedge failure (b) Slope of the landslide failure plane (in °) was obtained from the field survey.

town areas like Namchi, Ravangla, Yangang, Damthang, Turung, Mamring, Namthang, Jorthang, etc.

It is observed that some of the landslides have stabilised over time due to several reasons. Engineering structures such as retaining walls, gabions, crib walls (wire mesh filled with rocks), rock bolts, and anchors prevent landslides and help to stabilise the slope. However, these structures can sometimes exert additional pressure on an already disturbed land, potentially increasing the severity of the landslide hazard. Besides the abovementioned methods, several scientific and sustainable measures have been implemented in this region to prevent landslides. These include reshaping the slope by creating steps, lowering the slope angle, planting vegetation, and controlling drainage by installing canals or drains. Recently, the Sikkim government, with the help of local people, started constructing drains to revive dried springs and initiated rainwater harvesting to reduce water scarcity in the region, especially in South Sikkim. This also prevents sheetwash and reduces pore water pressure, which otherwise weakens the slope material. Additionally, step cultivation helps to stabilise the slope. This method of slope conservation has proven to be more effective in the study area than engineering structures. The Kopchey landslide is an example from the study area that demonstrates how sustainable preventive measures can effectively stabilise landslides. Some of the landslides of the region stabilised naturally over time.

**Impact of climate change on slope instability**

Climate change poses an urgent challenge, impacting ecologically fragile mountainous regions like Sikkim (Gupta, 2014). Climate and landslides operate on somewhat differing spatial and temporal scales, making it challenging to assess precisely how climate influences landslides (Gariano and Guzzetti, 2016). Climate change and its impact on the Himalayas have been studied by Tewari *et al*. (2017); Bhutiyani *et al*. (2007); Dimri and Dash (2012); and Diodato *et al*. (2012) to quote a few. Glacial retreat, increase in the number of glacial lakes, shrinking snow lines and extinction of different floral and fauna communities indicate severe climate change in the Sikkim Himalayas (Bhattacharya *et al*., 2012; Chowdhury *et al*., 2021b). In 2022, the annual mean land surface air temperature was 0.51°C higher than the long-term average of 1981–2010 in India (IMD, 2022), making this the fifth warmest year since 1901 (the warmest year was 2016, with an anomaly of +0.71°C). According to the State Action Plan on Climate Change (SAPCC, 2011), there is no change in maximum temperature in Sikkim, but the minimum temperature has increased by 2.5°C between 1957 and 2009. In this study, the MK test (Tables 2 and 3) reveals a distinct indication of an annual average temperature rise, particularly noticeable in the autumn and winter months, changing the normal trend and contributing to an escalation in post-monsoonal and winter precipitation.

Kakkar *et al*. (2022) have shown change in rainfall patterns in Sikkim since 2001. Based on the Long Period Average (LPA), rainfall was 108%, winter rainfall was 147%, and post-monsoon rainfall was 119% (IMD, 2022). Study of 33 years of data from Tadong station (East Sikkim), Click or tap here to enter text. 48% of the period experienced extreme wet conditions, which led to higher erosion and landslide activities (Das *et al*., 2017). Over 660 lives were tragically lost across various regions of the country due to the incidents of heavy rain, floods, and landslides in 2022 (IMD, 2023). A significant observation from the surveyed landslides indicates the reactivation of numerous large but dormant landslides, primarily triggered

due to the heightened precipitation levels in 2021 and 2022. Majority of the landslides observed are characterised as debris flow (Fig. 12a), underscoring their water-involvement, predominantly triggered by intense rainfall.

South Sikkim, the most drought-prone area of the state, is worst hit by climate change (Vishwakarma *et al*., 2017). The region is experiencing a growing issue of decline in springs, from 50% to 35%, due to climate change-induced shifts in precipitation patterns, including heightened rainfall intensity, reduced temporal spread, and diminished winter rain, coupled with other human-induced factors (Tambe *et al*., 2012). Namthang Automatic Weather Station (AWS), South Sikkim) reported a decrease in annual precipitation from 2533 mm to 1503 mm, turning most of the South Sikkim springs (the primary water sources in this region) from seasonal to dry. Initially, climate change induced warming boosts downstream water availability by melting of glaciers, but eventually this causes water scarcity (Basu *et al*., 2021). Field observations indicate that people have established settlements near streams or on the beds of dried spring channels during the dry period of 1990 to 2009. Subsequently, springs have been recharged due to heavy rainfall, but the obstructions created by the existing settlements, rendered the land susceptible to landslides. This, in turn, resulted in the instability of the slope and destruction of settlements in the path of the spring-induced channels. Heavy rainfall in 2021 resulted in the deviation of water flow through these channels from their original paths, primarily due to obstructions created by settlements, leading to seepage and slope subsidence (Fig. 13). Recognising the increased susceptibility of this area to landslides, the inhabitants were relocated to a safer location.

There was a decrease in Sikkim's annual rainfall of 250 mm from 1983 to 2009 (SAPCC, 2011). According to this report, 2001 to 2010 was the driest decade in the recent past, whereas 2008 and 2009 had the driest winter. During this study, 2003 was the driest year of that decade for both Namchi and Ravong (Fig. 14a and 14b). After that, the region received less rainfall for the next six years. This dry weather caused soil to shrink and crack, and when heavy rain occurred after the dry spell in 2010, the soil quickly absorbed the water, leading


**Figure 13.** Settlements obstructing the natural stream flow near Namchi have impeded the stream's course, leading to increased seepage and subsequent soil creep in the area.

to rapid expansion of the cracks. Expanded cracks diverted more water through them to saturate the soil and increased the pore water pressure, leading to landslides. Prolonged dry spells from 1999 to 2009, followed by sudden heavy rainfall in 2010, triggered landslides. These landslides involved massive amounts of regolith and had deep-seated roots. As a result, the landslide area increased (Fig. 6b) by more than 70% from 1999 ± 2 to 2009 ± 2, though the number of landslides increased by only 27% (Fig. 6a). In the following decade, the number of landslides almost doubled, despite a decrease in the landslide-affected area due to insufficient regolith. Post-2009, the region experienced several episodes of heavy rainfall, leading to frequent debris washouts. With inadequate time for regolith formation, this resulted in the formation of numerous shallow landslides, albeit smaller in scale.

As a result of increasing temperature trend proglacial lakes have predominantly undergone substantial enlargement, driven by accelerated melting and calving (Chowdhury *et al*., 2022). As mentioned, these lakes have the potential to breach, leading to Glacial Lake Outburst Floods (GLOFs). The effects of GLOF can propagate through significant distances ranging from tens to hundreds of kilometres and exhibit peak discharge and volume of several orders of magnitude greater than those associated with typical floods (Worni *et al*., 2014). Sattar *et al*. (2021) in their study depict the alarming condition of South Lhonak Lake in Sikkim, highlighting it as one of the rapidly expanding glacial lakes with potential to breach in the near future.

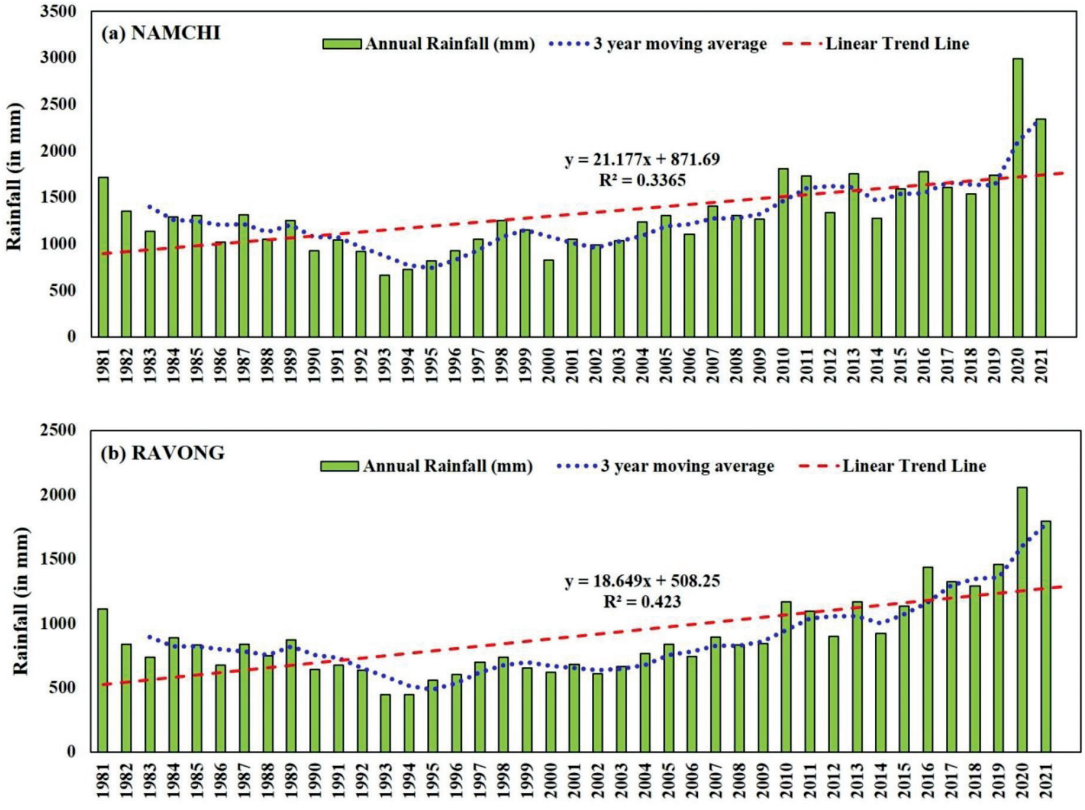


**Figure 14.** Annual rainfall distribution from 1989 to 2021 in (a) Namchi and (b) Ravong.

After two years of their study, on October 3-4, 2023, the glacial lake outburst from the South Lhonak Lake caused devastating floods downstream. The 1,200 MW Teesta III dam, the largest hydropower project in Sikkim located around 60 km downstream of the lake in Chungthang town (South district), was obliterated by the GLOF, resulting in widespread devastation in downstream areas and communities (Chettri, 2023). The floodwater travelled at an unimaginable velocity to reach the valley settlements of Singtam, covering 92 km in just 1 hour and with a gradient drop of 378 m. Within another hour, it reached further downstream up to the North Bengal region (Bhushan, 2023). This event resulted in extensive landslides along NH10 and bank erosion along the Teesta river, paralysing Sikkim for several days (Chauhan, 2023). The Gurudongmar Lake Complex, which combines four glacial lakes in North Sikkim, is another glacial lake in Eastern Himalaya that has the potential to generate another disaster associated with numerous landslides in the downstream region of Sikkim (Chowdhury *et al*., 2021a). Hence, these illustrate how climate change extremes can impact slope stability of any region beneath the glaciated zones (e.g. South Sikkim) or the foothill areas.

Figure 9 shows SEM images of samples from the Denchong landslide, offering high-resolution views for precise particle size and shape measurements. This information is crucial for understanding the granulometry of landslide materials, which can influence their stability and behaviour (Gresina *et al*., 2019; Wu *et al*., 2022; Xie *et al*., 2018). In the Denchong landslide (reactivated after the 2021 monsoon), sediment distribution from top to bottom exhibits a distinctive sorting pattern, transitioning from finer to coarser materials. At the upper reaches of the landslide, finer sediments, such as silts and clays, tend to predominate due to their susceptibility to erosion and transport (as shown in Fig. 9A – right panel). As the mass descends, the kinetic energy and gravitational forces involved in the landslide lead to selective sorting, causing the deposition of coarser sediments like sands (Fig. 9B) and gravels closer to the terminus of the landslide (Fig. 9C). The presence of water in the debris slide is evident in the collected samples, as depicted in Fig. 9A. Additionally, Fig. 9C reveals the presence of very fine plant stem-like features, suggesting biological weathering processes within the landslide material. These findings emphasise the impact of water and biological elements on the dynamics of debris slides, shedding light on the influence of a warm-moist climate on this landslide.

**Conclusions**

Prolonged dry weather from 1990 to 2009 desiccated the soils and made them non-cohesive, that made them crumble and break apart. This reduction in soil stability increases the likelihood of landslides. Steeper slopes, have less time for water to percolate into the ground because water moves rapidly downhill. This is another triggering factor of landslides in South Sikkim within this changing precipitation conditions. An increase in extreme rainfall events (like in 2021 and 2022) results in a quick runoff over steep slopes, causing erosion, washing away of topsoil and affecting slope stability. Human intervention is another cause of landslides in the study area. Road construction disturbs the natural equilibrium of the slopes by removing soil or rock from the base. More and more settlements like Namchi and Ravangla are coming up on the steep slopes of this hilly region to accommodate a growing population, which is creating more pressure on the geologically and seismically fragile land. Excavation, deforestation, and changes in drainage patterns due to settlement growth

remove the support provided by vegetation and soil cohesion, making slopes more susceptible to sliding.

Studying the vertical distribution of sediment through SEM also provides valuable insights into the mechanics and behaviour of landslides, aiding in assessing their triggers and potential impacts on the surrounding terrain. In subsequent research, integrating SEM with geological, geotechnical, and remote sensing data will enable a comprehensive analysis of landslides, facilitating informed evaluation of landslide risks and the development of probable mitigation strategies. With both rainfall and temperature exhibiting an upward trend, the findings from this study suggest a foreseeable increase in slope instability and subsequent landslides in the near future. The region encounters diverse weather conditions throughout the year, influenced by climate change. Summers are characterised by minimal rainfall, while autumn and winter experience above-average precipitation. Hot and dry summer contributes to heightened landslide activity, particularly during the post-monsoon season (especially in October-November). Further exploration of the seasonal variations in landslides is, therefore, crucial for understanding the influence of climate change on landslide occurrences. Additionally, the added weight of structures and human activities, such as mining and quarrying, can further destabilise slopes, triggering landslides. Proper planning, engineering enforcements, and land-use management will be crucial to mitigate these risks and ensure the safety of settlements in these landslide-prone areas.

**Acknowledgements**

The first author is thankful to the University Grants Commission, New Delhi, for granting the JRF and SRF. We would like to thank the Department of Geography at the North-Eastern Hill University (NEHU), Shillong, Meghalaya (India) and the Centre for the Study of Regional Development, Jawaharlal Nehru University, New Delhi (India), for different laboratory facilities. We also thank the central laboratory (i.e., Sophisticated Analytical Instrument Facility, SAIF) at NEHU for granting permission to utilise the Scanning Electron Microscopy (SEM) instrument. We conducted fieldwork in 2022 and 2023, and thus, we extend our heartfelt thanks to the local people of Sikkim for their invaluable help and support during fieldwork. We also acknowledge the United States Geological Survey (USGS) for providing the Landsat, Sentinel, and SRTM DEM data free of cost. We sincerely acknowledge the efforts of the anonymous reviewers and editor for their valuable suggestions that have enhanced our manuscript content and quality.

**References**

Ansari, T.A., Singh, K.H., Singh, T.N. and Tripathi, J.N., (2020) Stability analysis of road cut slope near Devprayag in Lesser Himalaya, India. *Journal of Earth System Science*: 129.

Baldis, C.T. and Liaudat, D.T. (2019) Rockslides and rock avalanches in the Central Andes of Argentina and their possible association with permafrost degradation. *Permafrost and Periglacial Processes*, John Wiley and Sons Ltd: 330–347.

Basu, R., Misra, G. and Sarkar, D. (2021) A remote sensing based analysis of climate change in Sikkim supported by evidence from the field. *Journal of Mountain Science* 18, 1256–1267.

Bera, A., Mukhopadhyay, B.P. and Das, D. (2019) Landslide hazard zonation mapping using multi-criteria analysis with the help of GIS techniques: a case study from Eastern Himalayas, Namchi, South Sikkim. *Natural Hazards,* 96: 935–959.

Bhasin, R., Aslan, G. and Dehls, J. (2023) Ground Investigations and Detection and Monitoring of Landslides Using SAR Interferometry in Gangtok, Sikkim Himalaya. *GeoHazards,* 4: 25–39.

Bhasin, R., Shabanimashcool, M., Hermanns, Reginald L, Hermanns, R L, Morken, O.A., Dehls, J.F. and Gupta, V. (2020) Back Analysis of Shear Strength Parameters of a Large Rock Slide in Sikkim Himalaya. *Journal of Rock Mechanics and Tunnelling Technology,* 26: 81–92.

Bhattacharya, S., Krishnaswamy, S. and Rao, C.K. (2012) Vulnerability of Sikkim to Climate Change and Strategies for Adaptation, In *Climate Change in Sikkim – Patterns, Impacts and Initiatives*. Gangtok: Information and Public Relations Department Government of Sikkim, 317–332.

Bhushan, C. (2023) GLOF's Sikkim shocker: Much before the flooding, local and green groups had flagged risks. *Times of India*. https://timesofindia.indiatimes.com/blogs/toi-edit-page/glofs-sikkim-shocker.

Bhutiyani, M.R., Kale, V.S. and Pawar, N.J. (2007) Long-term trends in maximum, minimum and mean annual air temperatures across the Northwestern Himalaya during the twentieth century. *Climate Change*, 85: 159–177.

Buller, S. (2014) *The Impacts of Climate Change on Geological Processes*. Undergraduate Dissertation towards B.Sc. Geography and Natural Hazards. 10.13140/2.1.3518.2729.

Calvin, K. and 85 others (2023) Climate Change 2023: Synthesis Report. In Lee, H. and Romero, J. (eds.) *Sixth Assessment Report of the Intergovernmental Panel on Climate Change* [Contribution of Working Groups I, II and III to the], IPCC, Geneva, Switzerland. https://doi.org/10.59327/IPCC/AR6-9789291691647

Chanda, A. (2019) Earthquake Risk Assessment in Sikkim through Geospatial Techniques. *International Journal of Technical Research & Science*, 4: 25–32.

Chauhan, A. (2023) Glacial Lake outburst flood kills 14 in Sikkim, 102 people missing: What is GLOF, and why does it happen? *The Indian Express*, October 6th, 2023.

Chettri, M. (2023) Who is responsible for Sikkim's glacial lake outburst flood?, *Frontline* https://frontline.thehindu.com/environment/article67453490.ece, October 25, 2023.

Chowdhury, A., De, S.K., Sharma, M.C. and Debnath, M. (2022) Potential Glacial Lake Outburst Flood Assessment in a changing environment, Chhombo Chhu Watershed, Sikkim Himalaya, India. *Geocarto International*. 37: 15627–15655.

Chowdhury, A., Kroczek, T., De, S.K., Vilímek, V., Sharma, M.C. and Debnath, M. (2021a) Glacial lake evolution (1962–2018) and outburst susceptibility of Gurudongmar Lake Complex in the Tista basin, Sikkim Himalaya, India. *Water* 13: 1–22.

Chowdhury, A., Sharma, M.C., Kumar De, S. and Debnath, M. (2021b) Glacier changes in the Chhombo Chhu Watershed of the Tista basin between 1975 and 2018, the Sikkim Himalaya, India. *Earth System Science Data* 13: 2923–2944.

Climate-data.org (2023) Namchi climate: Weather Namchi & temperature by month https://en.climate-data.org/asia/india/sikkim/namchi-24708.

Coe, J.A., Bessette-Kirton, E.K. and Geertsema, M. (2018) Increasing rock-avalanche size and mobility in Glacier Bay National Park and Preserve, Alaska detected from 1984 to 2016 Landsat imagery. *Landslides*, 15: 393–407.

Das, S.K., Avasthe, R., Sharma, P. and Sharma, K. (2017) Rainfall Characteristics Pattern and Distribution analysis at Tadong East Sikkim. *Indian Journal of Hill Farming*, 30: 326–330.

De, R. and Kayal, J.R. (2004) Seismic activity at the MCT in Sikkim Himalaya. *Tectonophysics*, 386, 243–248.

Devoli, G., Strauch, W., Chávez, G. and Høeg, K. (2007) A landslide database for Nicaragua: A tool for landslide-hazard management. *Landslides*, 4: 163–176.

Dhar, O.N., Soman, M.K. and Mulye, S.S. (1984) Rainfall over the southern slopes of the Himalayas and the adjoining plains during 'breaks' in the monsoon. *Journal of Climatology*, 4: 671–676.

Dikshit, A., Sarkar, R., Pradhan, B., Segoni, S. and Alamri, A.M. (2020) Rainfall induced landslide studies in Indian Himalayan region: A critical review. *Applied Sciences*, 10. https://

doi.org/10.3390/app10072466

Dimri, A.P. and Dash, S.K. (2012) Wintertime climatic trends in the western Himalayas. *Clim Change*, 111: 775–800.

Diodato, N., Bellocchi, G. and Tartari, G. (2012) How do Himalayan areas respond to global warming? *International Journal of Climatology*, 32: 975–982.

Dobrescu, C.F., Calarasu, E. and Stoica, M. (2011) Landslides analysis using geological, geotechnical and geophysical data from experimental measurements in Prahova County. *Urbanism. Architecture. Constructions*, 2(4): 55–62.

ENVIS Centre (2005) *Geology and Mineral Resources of Sikkim*. Ministry of Environment & Forest, Govt. of India. https://sikenvis.nic.in/Database/GSI_4420.aspx.

Fischer, E.M. and Knutti, R. (2015) Anthropogenic contribution to global occurrence of heavy-precipitation and high-temperature extremes. *Nature Climate Change*, 5(6): 560–564.

Fort, M., Cossart, E. and Arnaud-Fassetta, G. (2010) Hillslope-channel coupling in the Nepal Himalayas and threat to man-made structures: The middle Kali Gandaki valley. *Geomorphology*, 124: 178–199.

Ganepola, G.A.C. and Jayawardena, U. (2021) Effect of temperature increase for the occurrence of natural landslides, *Proceedings of the International Conference on Geotechnical Engineering*, organised by International Society for Soil Mechanics and Geotechnical Engineering, Colombo, Sri Lanka: pp. 391–394.

Gariano, S.L. and Guzzetti, F. (2016) Landslides in a changing climate. *Earth-Science Reviews*, 162: 227–252.

Gaunia, G. (2022) Landslide and its Management: A Study on Gangtok, Sikkim, India. *International Journal of Multidisciplinary Educational Research*, 11(7[6]): 20–29.

Gómez, D., García, E.F. and Aristizábal, E. (2023) Spatial and temporal landslide distributions using global and open landslide databases. *Natural Hazards*, 117: 25–55.

Government of Sikkim (2011) *District Profile: District Namchi, Government of Sikkim, India*. https://namchi.nic.in/about-district/district-profile/ (accessed 3.29.23).

Gresina, F., Páles, M., Jakab, G., Udvardi, B., Varga, G., Falus, G., Szalai, Z. and Király, C. (2019). Particle size and shape results from a landslide area in Kulcs, Hungary. (Abstract), *EGU General Assembly*, organised by the European Geoscience Union, Vienna, Austria.

Gupta, K. (2014) The Impact of Climate Change on Sikkim, in: *Climate Change and the Himalayas*, 118: 2.

Gupta, V., Mahajan, A.K. and Thakur, V.C. (2015) A study on landslides triggered during Sikkim earthquake of September 18, 2011. *Himalayan Geology*, 36: 81–90.

Hamal, K., Sharma, S., Talchabhadel, R., Ali, M., Dhital, Y.P., Xu, T. and Dawadi, B. (2021) Trends in the diurnal temperature range over the southern slope of Central Himalaya: Retrospective and prospective evaluation. *Atmosphere*, MDPI, Basel, Switzerland, 12, 1683. https://doi.org/10.3390/atmos12121683.

IMD (2022) *Statement on Climate of India during 2022*. India Meteorological Department (Climate Research and Services), Ministry of Earth Sciences, Govt. of India, 11p.

IMD (2023) *Annual Report, India Meteorological Department*, Ministry of Earth Sciences, Govt. of India, 241p.

Jaboyedoff, M., Michoud, C., Derron, M.H., Voumard, J., Leibundgut, G., Sudmeier-Rieux, K., Michoud, C., Nadim, F. and Leroi, E. (2016) Human-Induced Landslides: Toward the Analysis of Anthropogenic Changes of the Slope Environment. In Avresa S., Cascini L., Picarelli L. and Scavia C (eds) *Landslides and Engineered Slopes. Experience, Theory and Practice*. Taylor and Francis Inc.: 217–232.

Jana, M.M. (2002) Application of Remote Sensing in the Study of Geomorphic Processes and Landforms in Piedmont Zone of Darjeeling Sub-Himalaya. *Journal of the Indian Society of Remote Sensing*, 30: 61–72. https://doi.org/10.1007/BF02989977.

Jones, S., Kasthurba, A.K., Bhagyanathan, A. and Binoy, B. V. (2021) Impact of anthropogenic activities on landslide occurrences in southwest India: An investigation using spatial models. *Journal of Earth System Science*, 130(70): 18p. https://doi.org/10.1007/s12040-021-01566-6

Kakkar, A., Rai, P.K., Mishra, V.N. and Singh, P. (2022) Decadal trend analysis of rainfall patterns of past 115 years and its impact on Sikkim, India. *Remote Sensing Applications: Society and Environment*, 26: 100738. https://doi.org/10.1016/j.rsase.2022.100738

Kaur, H., Gupta, S., Parkash, S., Thapa, R., Gupta, A., Khanal, G.C., 2019. Evaluation of landslide susceptibility in a hill city of Sikkim Himalaya with the perspective of hybrid modelling techniques. *Annals of GIS*, 25(11): 1–20.

Kellett, D., Grujic, D., Mottram, C. and Mukul, M. (2014) Virtual field guide for the Darjeeling-Sikkim Himalaya, India. *Journal of the Virtual Explorer*, 47(5): 1–38. https://doi.org/10.3809/jvirtex.2014.00344

Kendall, M.G. (1948) *Rank Correlation Methods*. Charles Griffin and Co. Ltd., London, 202p.

Kirschbaum, D., Kapnick, S.B., Stanley, T. and Pascale, S. (2020) Changes in Extreme Precipitation and Landslides Over High Mountain Asia. *Geophysical Research Letters*, 47(4): 1–9. https://doi.org/10.1029/2019GL085347

Koley, B., Nath, A., Saraswati, S., Bandyopadhyay, K. and Ray, B.C. (2019) Assessment of Rainfall Thresholds for Rain-Induced Landslide Activity in North Sikkim Road Corridor in Sikkim Himalaya, India. *Journal of Geography, Environment and Earth Science International*, 19(3): 1–14. https://doi.org/10.9734/jgeesi/2019/v19i330086

Kumar, A., Asthana, A.K.L., Priyanka, R.S., Jayangondaperumal, R., Gupta, A.K. and Bhakuni, S.S. (2017) Assessment of landslide hazards induced by extreme rainfall event in Jammu and Kashmir Himalaya, northwest India. *Geomorphology*, 284: 72–87.

Lee, W.L., Martinelli, M. and Shieh, C.L. (2021) An investigation of rainfall-induced landslides from the pre-failure stage to the post-failure stage using the Material Point Method. *Frontiers in Earth Science*, 9(764393): 1–13. https://doi.org/ 10.3389/feart.2021.764393

Mann, H.B. (1945) Nonparametric Tests Against Trend. *Econometrica*, 13: 245–259.

Martha, T.R., Roy, P., Govindharaj, K.B., Kumar, K.V., Diwakar, P.G. and Dadhwal, V.K. (2015) Landslides triggered by the June 2013 extreme rainfall event in parts of Uttarakhand state, India. *Landslides*, 12(1): 135–146. https://doi.org/10.1007/s10346-014-0540-7

Merzdorf, J. (2020) Climate Change Could Trigger More Landslides in High Mountain Asia. *Global Climate Change: Vital Signs of the Planet*, https://climate. nasa.gov/news/2951/climate-change-could-trigger-more-landslides-in-high-mountain-asia/ (accessed 3.28.23).

Mondal, S. and Mandal, S. (2019) Landslide susceptibility mapping of Darjeeling Himalaya, India using index of entropy (IOE) model. *Applied Geomatics*, 11: 129–146. https://doi.org/10.1007/s12518-018-0248-9

Mottram, C.M., Argles, T.W., Harris, N.B.W., Parrish, R.R., Horstwood, M.S.A., Warren, C.J. and Gupta, S. (2014) Tectonic interleaving along the Main Central Thrust, Sikkim Himalaya. *Journal of the Geological Society*, London, 171(2): 255–268.

Pradhan, S., Toll, D.G., Rosser, N.J. and Brain, M.J. (2022) An investigation of the combined effect of rainfall and road cut on landsliding. *Engineering Geology*, 307: 1–16. https://doi.org/10.1016/j.enggeo.2022.106787

Priya, R.K., Rajan, R.K., Tewari, V.C. and Ranjan, R. (2019) Permian Tethyan transgression in Sikkim-Darjeeling Himalaya with special reference to the Paleoclimatic event. *Bulletin of Nepal Geological Society*, 36: 233–240.

Rawat, M. S., Joshi, V. and Sundriyal, Y.P. (2017) Slope stability analysis in a part of East Sikkim, using Remote Sensing & GIS. In: *Proceedings of the 2nd International Conference on Next Generation Computing Technologies*, *2016*, Dehradun, India, Institute of Electrical and Electronics Engineers: 51–60. https:// doi.org/ 10.1109/NGCT.2016.7877389.

Rawat, Manmohan Singh, Dobhal, R., Joshi, V. and Sundriyal, Y. (2017) Landslide Hazard Zonation Study in Eastern Indian Himalayan Region. *International Journal of Georesources and Environment*, 3(1): 35–46.

Rosin, P.L. and Hervás, J. (2005) Remote sensing image thresholding methods for determining landslide activity. *International Journal of Remote Sensing*, 26: 1075–1092. https://doi.org/10.1080/01431160512331330481

Sangeeta, S. and Singh, S. (2023) Influence of anthropogenic activities on landslide susceptibility: A case study in Solan district, Himachal Pradesh, India. Journal of Mountain Science, 20(2): 429–447. https://doi.org/10.1007/S11629-022-7593-1.

SAPCC, 2011. *The Sikkim State Action Plan on Climate Change, Report*. Govt. of Sikkim, 138p.

Sarkar, K. and Mandal, S. (2021) Assessment of Landslide risk using BLR and AHP for South Sikkim Himalaya. *India. Disaster Advances*, 14: 1–25.

Sathyanathan, R., Bhutia, S.Y., Jyrwa, K.L. and Jewel, T.R. (2020) Precipitation analysis for the East and South districts of Sikkim, India. In: *3rd International Conference on Advances in Mechanical Engineering*, IOP Conference Series: Materials Science and Engineering, IOP Publishing Ltd., 912: 1–11. https://doi.org/10.1088/1757-899X/912/6/062071

Sattar, A., Goswami, A., Kulkarni, A. V., Emmer, A., Haritashya, U.K., Allen, S., Frey, H. and Huggel, C. (2021) Future Glacial Lake Outburst Flood (GLOF) hazard of the South Lhonak Lake, Sikkim Himalaya. *Geomorphology*, 388: 1–19. https://doi.org/10.1016/j.geomorph.2021.107783

Schaller, G.B. (1977) *Mountain Monarchs: Wild Goat and Sheep of the Himalaya*. University of Chicago Press, Chicago: 425p.

Sen, P.K. (1968) Estimates of the Regression Coefficient Based on Kendall's Tau. *Journal of the American Statistical Association*, 63(324): 1379–1389.

Sharma, I., Pradhan, P. and Tewari, V.C. (2015) Proposed Geopark (Stromatolite Fossil Park) Development at Mamley area South Sikkim with emphasis on promotion of Geotourism in Sikkim Himalaya (Abstract). In The *30th Himalaya-Karakoram-Tibet Workshop, at: Wadia Institute of Himalayan Geology*, Dehradun, Uttarakhand, India.

Sharma, S.P., Anbarasu, K., Gupta, S. and Sengupta, A. (2010) Integrated very low-frequency EM, electrical resistivity, and geological studies on the Lanta Khola landslide, North Sikkim, India. *Landslides*, 7(1): 43–53.

Singh, T. and Bajpai, U. (1990) On some plant fossils from Gondwana equivalent sediments of Eastern Himalaya. *The Palaeobotanist*, 37(1–3): 284–291.

Snook, P., Hermanns, R.L., Czekirda, J., Myhra, K.S., Gosse, J.C. and Etzelmüller, B. (2021) Permafrost as a first order control on long-term rock-slope deformation in (Sub-)Arctic Norway. *Quaternary Science Reviews*, 251. 10.1016/j.quascirev.2020.106718

Tambe, S., Kharel, G., Arrawatia, M.L., Kulkarni, H., Mahamuni, K. and Ganeriwala, A.K. (2012) Reviving dying springs: Climate change adaptation experiments from the Sikkim Himalaya. *Mountain Research and Development*, 32(1): 62–72. https://doi.org/10.1659/MRD-JOURNAL-D-11-00079.1.

Tewari, V.P., Verma, R.K. and von Gadow, K. (2017) Climate change effects in the Western Himalayan ecosystems of India: evidence and strategies. *Forest Ecosystems*, 4(13): 1–9. https://doi.org/10.1186/s40663-017-0100-4

Tohari, A., 2018. Study of rainfall-induced landslide: A review. In *Global Colloquium on Geosciences and Engineering 2017*, IOP Conference Series: Earth and Environmental Science, IOP Publishing Ltd., 118: 1–6. https://doi.org/10.1088/1755-1315/118/1/ 012036

Tourism and Civil Aviation Department (2020) *Namchi: Popular Places — Sikkim Tourism*. Govt. of Sikkim. https://www.sikkimtourism.gov.in /Public/Places to Go/Popular Place Details/PA20A006 (accessed 3.29.23).

Velayudham, J., Kannaujiya, S., Sarkar, T., Champati ray, P.K., Taloor, A.K., Singh Bisht, M.P., Chawla, S. and Pal, S.K. (2021) Comprehensive study on evaluation of

Kaliasaur Landslide attributes in Garhwal Himalaya by the execution of geospatial, geotechnical and geophysical methods. *Quaternary Science Advances*, 3: 1–14. https://doi.org /10.1016/j.qsa.2021.100025.

Vishwakarma, C.A., Asthana, H., Singh, D., Pant, M., Sen, R. and Mukherjee, S. (2017) GIS Based Bi-variate Statistical Approach for Landslide Susceptibility Mapping of South District, Sikkim. *International Journal of Innovative Research in Science, Engineering and Technology*, 6(7): 13661–13674. https://doi.org/10.15680/IJIRSET.2017.0607123.

Worni, R., Huggel, C., Clague, J.J. and Schaub, Y. (2014) Coupling glacial lake impact, dam breach, and flood processes: A modelling perspective. *Geomorphology*, 224: 161–176. 10.1016/j.geomorph.2014.06.031.

Wu, Y., Huang, S., Liu, K., Zhang, Q., Pan, H., 2022. Study on Physical and Mechanical Characteristics of Shear Band in Jinpingzi Landslide Region II. *Frontiers in Physics*, 10: 1–8. https://doi.org/10.3389/fphy.2022.857274

Xie, W. li, Li, P., Zhang, M. sheng, Cheng, T. e. and Wang, Y. (2018) Collapse behavior and microstructural evolution of loess soils from the Loess Plateau of China. *Journal of Mountain Science*, 15(8): 1642–1657. https://doi.org/10.1007/s11629-018-5006-2.

Yadava, A.K., Yadav, R.R., Misra, K.G., Singh, J. and Singh, D. (2015) Tree ring evidence of late summer warming in Sikkim, Northeast India. *Quaternary International*, 371: 175–180. https://doi.org/10.1016/j.quaint.2014.12.067

Zhang, J., Liu, R., Deng, W., Khanal, N.R., Gurung, D.R., Murthy, M.S.R. and Wahid, S. (2016) Characteristics of landslide in Koshi River Basin, Central Himalaya. *Journal of Mountain Science*, 13(10): 1711–1722. https://doi.org/10.1007/S11629-016-4017-0.

Date received: 11 August 2023
Date accepted after revision: 31 December 2023